

# Inflation Driven by Non-Linear Electrodynamics

H. B. Benaoum,<sup>1,\*</sup> Genly Leon,<sup>2,3,†</sup> A. Övgün,<sup>4,‡</sup> and H. Quevedo<sup>5,6,§</sup>

<sup>1</sup> *Department of Applied Physics and Astronomy,  
University of Sharjah, United Arab Emirates*

<sup>2</sup> *Departamento de Matemáticas, Universidad Católica del Norte,  
Avda. Angamos 0610, Casilla 1280 Antofagasta, Chile*

<sup>3</sup> *Institute of Systems Science, Durban University of Technology, PO Box 1334, Durban 4000, South Africa*

<sup>4</sup> *Physics Department, Eastern Mediterranean University,  
Famagusta, 99628 North Cyprus via Mersin 10, Turkey.*

<sup>5</sup> *Instituto de Ciencias Nucleares, Universidad Nacional Autónoma de México, AP 70543, Ciudad de México 04510, Mexico.*

<sup>6</sup> *Dipartimento di Fisica and ICRANet, Università di Roma “La Sapienza”, I-00185 Roma, Italy.*

(Dated: March 25, 2024)

We investigate the inflation driven by a non-linear electromagnetic field based on a NLED lagrangian density  $\mathcal{L}_{nled} = -\mathcal{F}f(\mathcal{F})$ , where  $f(\mathcal{F})$  is a generalized functional depending on  $\mathcal{F}$ . We first formulate an  $f$ -NLED cosmological model with a more general functional  $f(\mathcal{F})$  and show that all NLED models can be expressed in this framework; then, we investigate in details two interesting examples of the functional  $f(\mathcal{F})$ . We present our phenomenological model based on a new Lagrangian for NLED. Solutions to the field equations with the physical properties of the cosmological parameters are obtained. We show that the early Universe had no Big-Bang singularity, which accelerated in the past. We also investigate the qualitative implications of NLED by studying the inflationary parameters, like the slow-roll parameters, spectral index  $n_s$ , and tensor-to-scalar ratio  $r$  and compare our results with observational data. Detailed phase-space analysis of our NLED cosmological model is performed with and without matter source. As a first approach, we consider the motion of a particle of unit mass in an effective potential. Our systems correspond to fast-slow systems for physical values of the electromagnetic field and the energy densities at the end of inflation. We analyze a complementary system using Hubble-normalized variables to investigate the cosmological evolution previous to the matter-dominated Universe.

PACS numbers: 98.80.Bp; 11.10.Lm

Keywords: Cosmology; Inflation; Nonlinear electrodynamics; Early universe, Acceleration

## I. INTRODUCTION

The inflationary paradigm [1–6] of the early Universe has become a crucial part of the standard cosmological model since it has received tremendous support by the latest observational data [7–10]. According to this scenario, the early Universe underwent an accelerated expansion that could solve several puzzles of the hot Big-Bang cosmology such as the flatness problem, the horizon problem as well as the origin of the large scale structures of the Universe [9, 11]. The simplest approach to describe the inflationary era is to use a canonical scalar field with self-interacting potential. A variety of inflationary models have been proposed such as non-minimal Higgs inflation [12], Starobinsky inflation [1] and others [13–61]. Despite the impressive success of inflation, the standard cosmological model has a cosmological singularity at a finite time in the past where the curvature and energy density are not finite [62, 63]. Some proposals of cosmological models are free of any singularities based on various distinct mechanisms. For an incomplete list of non-singular cosmological models see [66–69].

Another approach developed by Born and Infeld (BI) [70–72] as a way to cure the divergences of self-energy of charged particles, is to replace the original Maxwell Lagrangian by a non-linear electrodynamics (NLED) Lagrangian. Similarly, Plebanski studied different models of NLED Lagrangians and proved that the BI model satisfies physically acceptable requirements [73]. There are various applications of NLED in the literature, including cosmology and astrophysics [74–81], high power laser technology, plasma physics, nonlinear optics [82–85] and the

---

\*Electronic address: [hbenauom@sharjah.ac.ae](mailto:hbenauom@sharjah.ac.ae)

†Electronic address: [genly.leon@ucn.cl](mailto:genly.leon@ucn.cl)

‡Electronic address: [ali.ovgun@emu.edu.tr](mailto:ali.ovgun@emu.edu.tr); <https://aovgun.weebly.com/>

§Electronic address: [quevedo@nucleares.unam.mx](mailto:quevedo@nucleares.unam.mx)

field nonlinear exponential growth due to chiral plasma instability [86]. In this framework, the standard cosmological model based on Friedmann-Lemaître-Robertson-Walker (FLRW) geometry with the non-linear electromagnetic field as its source, leads to a cosmological model without primordial singularity. Other interesting NLED models have been introduced in the literature [87–113].

In [113], Benaoum and Övgün have proposed a phenomenologically viable cosmological model based on NLED that could address some open cosmological problems such as the absence of primordial singularity, an early acceleration of the Universe, and the generation of matter-antimatter. One of the exciting features of nonlinearity is the removal of the initial singularity. We have assumed that a stochastic magnetic field background fills the Universe. Magnetic fields are believed to have played a crucial role in the evolution of the Universe, and it is not surprising that our Universe is teeming with magnetic fields. Magnetic fields are present everywhere in our Universe [114, 115]. Furthermore, a lower bound on the strength of the magnetic field of the order of  $B \geq 3 \times 10^{-16} G$  has been obtained for intergalactic magnetic fields [116] whereas the Planck satellite in 2015 gives an upper limit to be of the order of  $B < 10^{-9} G$  [117]. However, very little is known about the existence and origin of magnetic fields in the early Universe [118–120]. Finding primordial magnetic fields would transform our understanding of how our Universe evolved.

Our main aim is to study a new generalized case of NLED Lagrangian density which can be important in the very early Universe, leading to the avoidance of the singularity. To do so, in the present work, we investigate the inflation driven by a non-linear electromagnetic field based on a NLED lagrangian density  $\mathcal{L}_{nled} = -\mathcal{F}f(\mathcal{F})$ , where  $f(\mathcal{F})$  is a generalized functional depending on  $\mathcal{F}$ . The non-linearity is encoded in the generalized functional  $f(\mathcal{F})$ . We first formulate an  $f$ -NLED cosmological model with a more general functional  $f(\mathcal{F})$  and show that all NLED models can be expressed in this framework; then, we investigate in details two interesting examples of functional  $f(\mathcal{F})$ . The outline of the paper is as follows. In section II, we present our phenomenological model based on a new Lagrangian for NLED. Solutions to the field equations with the physical properties of the cosmological parameters are obtained. Here, we show that the early Universe had no Big-Bang singularity and tended to accelerate in the past. We also investigate the qualitative implications of NLED by studying the inflationary parameters, like the slow-roll parameters, spectral index  $n_s$ , and tensor-to-scalar ratio  $r$  and compare our results with observational data. Detailed phase-space analysis of our NLED cosmological model is performed in section III with and without matter source. Finally, we devote section IV to our conclusions.

## II. GENERAL RELATIVITY COUPLED TO NON-LINEAR ELECTRODYNAMICS

The action of Einstein's gravity coupled with NLED is given as follows:

$$S = \int d^4x \sqrt{-g} \left( \frac{1}{2\kappa^2} R + \mathcal{L}_{nled} \right), \quad (1)$$

where  $R$  is the Ricci scalar and  $\kappa^{-1} = M_p$  is the reduced Planck mass. In this work, we will use geometrized units, where  $8\pi G = 1, c = 1$  with the exception of inflationary setup where the reduced Planck mass  $M_p$  is inserted in the equations.

In general, the NLED Lagrangian can be expressed as a functional of  $\mathcal{F} = \frac{1}{4}F_{\mu\nu}F^{\mu\nu}$  and  $\mathcal{G} = \frac{1}{4}F_{\mu\nu}\tilde{F}^{\mu\nu}$ , where  $F_{\mu\nu}$  is the field strength tensor and  $\tilde{F}_{\mu\nu}$  is its dual. Since the classical Maxwell theory is valid in the low-energy/weak-coupling limit, the NLED Lagrangian reduces to the Maxwell one, i.e.  $\mathcal{L} = -\mathcal{F}$  in the corresponding limit. Here, we restrict ourselves to the case of a NLED Lagrangian depending on the electromagnetic field strength invariant  $\mathcal{F}$  where the classical Maxwell's Lagrangian density is replaced by

$$\mathcal{L}_{nled} = -\mathcal{F}f(\mathcal{F}), \quad (2)$$

where  $f \equiv f(\mathcal{F})$  is the generalized functional depending on  $\mathcal{F}$ .

Variation of the action for the metric and the NLED fields leads to the following field equations,

$$R_{\mu\nu} - \frac{1}{2}g_{\mu\nu}R = \kappa^2 T_{\mu\nu}, \quad (3)$$

and

$$\partial_\mu \left( \sqrt{-g} \frac{\partial \mathcal{L}_{nled}}{\partial \mathcal{F}} F^{\mu\nu} \right) = 0. \quad (4)$$

where  $T_{\mu\nu}$  is the energy-momentum tensor of the NLED fields,

$$T^{\mu\nu} = H^{\mu\lambda} F^\nu_\lambda - g^{\mu\nu} \mathcal{L}_{nled}, \quad H^{\mu\lambda} = \frac{\partial \mathcal{L}_{nled}}{\partial F_{\mu\lambda}} = \frac{\partial \mathcal{L}_{nled}}{\partial \mathcal{F}} F^{\mu\lambda}. \quad (5)$$

From the above NLED Lagrangian density, the energy-momentum tensor can be written as:

$$T^{\mu\nu} = -(f + \mathcal{F} f_{\mathcal{F}}) F^{\mu\lambda} F^\nu_\lambda + g^{\mu\nu} \mathcal{F} f, \quad (6)$$

where  $f_{\mathcal{F}} = \frac{df}{d\mathcal{F}}$ . The energy density  $\rho$  and pressure  $p$  can be obtained as follows:

$$\begin{aligned} \rho_{nled} &= \mathcal{F} f - E^2 (f + \mathcal{F} f_{\mathcal{F}}) \\ p_{nled} &= -\mathcal{F} f + \frac{2B^2 - E^2}{3} (f + \mathcal{F} f_{\mathcal{F}}). \end{aligned} \quad (7)$$

Assuming that the stochastic magnetic fields are the cosmic background with the wavelength smaller than the curvature, we can use the averaging of EM fields which are sources in GR, to obtain a FLRW isotropic spacetime [121]. The averaged EM fields are as follows:

$$\langle \mathbf{E} \rangle = \langle \mathbf{B} \rangle = 0, \quad \langle E_i B_j \rangle = 0, \quad (8)$$

$$\langle E_i E_j \rangle = \frac{1}{3} E^2 g_{ij}, \quad \langle B_i B_j \rangle = \frac{1}{3} B^2 g_{ij}.$$

where the averaging brackets  $\langle \rangle$  is used for simplicity.

In what follows, we consider the case where the electric field vanishes, i.e.  $E^2 = 0$ , and a non-zero averaged magnetic field leads to a magnetic Universe. Such a purely magnetic case turns out to be relevant in cosmology, where the charged primordial plasma screens the electric field, and the Universe's magnetic field is frozen for the magnetic properties to occur.

The energy density and pressure for  $E^2 = 0$  becomes

$$\begin{aligned} \rho &= \mathcal{F} f \\ p &= \frac{1}{3} \mathcal{F} (f + 4\mathcal{F} f_{\mathcal{F}}), \end{aligned} \quad (9)$$

where  $\mathcal{F} = \frac{1}{2} B^2$ .

In [113], Benaoum and Övgün have proposed a functional depending on two real parameters  $\alpha$  and  $\beta$  given by:

$$f(\mathcal{F}) = \frac{1}{(\beta \mathcal{F}^\alpha + 1)^{1/\alpha}}, \quad (10)$$

where  $\beta \mathcal{F}^\alpha$  is dimensionless,  $\beta$  is the non-linearity parameter and the usual Maxwell's electrodynamics Lagrangian is recovered when  $\beta = 0$ .

The energy density and pressure are:

$$\begin{aligned} \rho_B &= \frac{\mathcal{F}}{(\beta \mathcal{F}^\alpha + 1)^{1/\alpha}} \\ p_B &= -\frac{\mathcal{F}}{(\beta \mathcal{F}^\alpha + 1)^{1/\alpha}} + \frac{2}{3} \frac{B^2}{(\beta \mathcal{F}^\alpha + 1)^{1+1/\alpha}}. \end{aligned} \quad (11)$$

The equation of state (EoS) satisfied by this NLED Lagrangian is:

$$p_B = \frac{1}{3} \rho_B (1 - 4\beta \rho_B^\alpha) \quad (12)$$

which clearly shows that when the non-linearly is turned-off (i.e.  $\beta = 0$ ), it reduces to a radiation EoS.

In the context of inflationary paradigm, we choose the background spacetime to be described by a homogeneous, isotropic and spatially flat metric, which takes the following form:

$$ds^2 = -dt^2 + a(t)^2 [dr^2 + r^2 (d\theta^2 + \sin^2 \theta d\phi^2)], \quad (13)$$

where  $a(t)$  is the scale factor that governs the evolution of the spacetime.

For such a metric, the Friedmann equations can be easily computed, which results in,

$$\begin{aligned} H^2 &= \left(\frac{\dot{a}}{a}\right)^2 = \frac{1}{3} \rho_B \\ 3\frac{\ddot{a}}{a} &= -\frac{1}{2}(\rho_B + 3p_B) \end{aligned} \quad (14)$$

where  $H = \dot{a}/a$  is the Hubble parameter.

Using the conservation of the energy-momentum tensor  $\nabla^\mu T_{\mu\nu} = 0$ , the continuity equation of the NLED is derived as,

$$\dot{\rho}_B + 3H(\rho_B + p_B) = 0 \quad (15)$$

The above equation can be readily integrated, yielding the following relation between the electromagnetic field strength  $\mathcal{F}$  and the scale factor  $a$ ,

$$\mathcal{F} = \mathcal{F}_{end} \left(\frac{a_{end}}{a}\right)^4 = \mathcal{F}_0 \left(\frac{a_0}{a}\right)^4 = 2B^2. \quad (16)$$

It follows that:

$$B = B_{end} \left(\frac{a_{end}}{a}\right)^2 = B_0 \left(\frac{a_0}{a}\right)^2, \quad (17)$$

where  $a_{end}$  ( $a_0$ ) is the value scale factor and  $\mathcal{F}_{end} = \frac{1}{2}B_{end}^2$  ( $\mathcal{F}_0 = \frac{1}{2}B_0^2$ ) is the value of the electromagnetic field at the end of inflation (at the current time) respectively.

Notice that in geometrized units all the quantities have dimension of a power of length  $[L]$ . In this system of units, a quantity which has  $L^n T^m M^p$  in ordinary units converse to  $L^{n+m+p}$ . To recover nongeometrized units, we have to use the conversion factor  $c^m (8\pi G/c^2)^p$ . Thus, the dimension of  $B_0$  and  $H_0$  is  $[L^{-1}]$  in geometrized units and the conversion factors are  $1\text{Gauss} = 1.44 \times 10^{-24} \text{cm}^{-1}$  and  $H_0 = h 1.08 \times 10^{-30} \text{cm}^{-1}$ , where  $h = (67.4 \pm 0.5) \times 10^{-2}$  and  $N_{\text{eff}} = 2.99 \pm 0.17$  according to the Planck 2018 results [122, 123]. Then, we are dealing with magnetic fields of the order  $10^{-40} \text{cm}^{-1} \lesssim B_0 \lesssim 10^{-33} \text{cm}^{-1}$  in the present epoch. Then, we can obtain

$$\mathcal{F}_{end} = \frac{1}{2}B_{end}^2 = \frac{1}{2}B_0^2 \left(\frac{a_{end}}{a_0}\right)^{-4} = \frac{1}{2}B_0^2 (1+z_{end})^4 \quad (18)$$

where we have introduce the redshift  $z$ , such that

$$1+z = \frac{a_0}{a}, \quad 1+z_{end} = \frac{a_0}{a_{end}}, \quad (19)$$

where  $a_0$  is the present value of the scale factor (we assume  $a_0 \neq 1$ ),  $a_{end} = a(t_{end})$  is the scale factor evaluated at the end of inflation, and  $z_{end}$  is the redshift at the end of inflation.

Assuming that a Grand Unified Theory (GUT) describes Nature, the grand unified epoch was the period in the evolution of the early Universe that followed the Planck epoch, beginning about  $10^{-43}$  seconds after the Big Bang, in which the temperature of the Universe was comparable to the characteristic temperatures of the GUT. If the grand unification energy is taken as  $10^{15}$  GeV, this corresponds to temperatures above  $10^{27} \text{K}$ . During this period, three out of four fundamental interactions, electromagnetism, the strong, and the weak, were unified into the electronuclear force. Gravity had separated from the electronuclear force at the end of the Planck era. During the grand unification epoch, physical characteristics such as mass, charge, flavour, and colour were meaningless. The GUT epoch ended at approximately  $10^{-36}$  seconds after the Big Bang. At this point, several key events

took place. The strong force separated from the other fundamental forces. It is possible that some part of this decay process violated the conservation of baryon number and gave rise to a small excess of matter over antimatter. It is also believed that this phase transition triggered the cosmic inflation process that dominated the Universe's evolution during the following inflationary epoch. The inflationary epoch lasted from  $10^{-36}$  seconds after the conjectured Big Bang singularity to sometime between  $10^{-33}$  and  $10^{-32}$  seconds after the singularity. During the inflationary period, the universe continued to expand, but at a slower rate. Then, we can take as characteristic values for  $z_{end}$  at Grand Unified Theory (GUT) scale is  $z_{end} \simeq z_{GUT} \simeq 10^{28}$ , or two orders of magnitude less, say  $z_{end} \simeq 10^{-2} z_{GUT} \simeq 10^{26}$ , or  $z_{end} \simeq 10^{10}$ , i.e. two orders of magnitude above nucleosynthesis. Hence, for the theoretical prior  $z_{end} \simeq z_{GUT}$ , we have  $5 \times 10^{31} \text{cm}^{-2} \lesssim \mathcal{F}_{end} \lesssim 5 \times 10^{45} \text{cm}^{-2}$ . For the theoretical prior  $z_{end} \simeq 10^{10}$ , we have  $5 \times 10^{-41} \text{cm}^{-2} \lesssim \mathcal{F}_{end} \lesssim 5 \times 10^{-27} \text{cm}^{-2}$ . Taking a prior  $z_{end} \simeq 10^{-2} z_{GUT} \simeq 10^{26}$  as an educated guess we have  $5 \times 10^{23} \text{cm}^{-2} \lesssim \mathcal{F}_{end} \lesssim 5 \times 10^{37} \text{cm}^{-2}$ .

In terms of redshift we have

$$\mathcal{F}(z) = \frac{1}{2} B_0^2 (1+z)^4 = \mathcal{F}_{end} \left( \frac{1+z}{1+z_{end}} \right)^4. \quad (20)$$

The acceleration expansion during inflation ends (i.e.  $\ddot{a} = 0$ ) when the energy density of the electromagnetic field energy density reaches the value

$$\rho_{end} = \frac{1}{(2\beta)^{1/\alpha}}. \quad (21)$$

One can immediately find that the energy density and the pressure in terms of the scale factor  $a$  as,

$$\rho_B = \frac{\rho_0}{\left(1 + \left(\frac{a}{a_{end}}\right)^{4\alpha}\right)^{1/\alpha}}, \quad p_B = \rho_0 \frac{-1 + \frac{1}{3} \left(\frac{a}{a_{end}}\right)^{4\alpha}}{\left(1 + \left(\frac{a}{a_{end}}\right)^{4\alpha}\right)^{1+1/\alpha}}, \quad (22)$$

where  $\rho_0 = \rho_B(a=0)$  is the energy density at the early phase of the Universe.

### A. No Early/Late Singularity

In this section, we will demonstrate that it is indeed possible to have an early/late Universe, described by our NLED model coupled to gravity, with no cosmological singularity. For this purpose, we study the behavior of the energy density, the pressure, the Ricci scalar curvature, the Ricci tensor squared and the Kretschmann scalar in the limits of  $a(t) \rightarrow 0$  and  $a(t) \rightarrow \infty$ . From the above equations, it follows,

$$\lim_{a(t) \rightarrow 0} \rho_B(t) = \beta^{-1/\alpha}, \quad \lim_{a(t) \rightarrow 0} p_B(t) = -\beta^{-1/\alpha}, \quad (23)$$

$$\lim_{a(t) \rightarrow \infty} \rho_B(t) = \lim_{a(t) \rightarrow \infty} p_B(t) = 0. \quad (24)$$

It is worth noticing that the non-linearity  $\beta$  is related to the energy density of the NLED field at the early epoch of the Universe,

$$\rho_0 = \rho_B(a=0) = \beta^{-1/\alpha}. \quad (25)$$

Such a maximum energy density allowed in electromagnetic fields could solve many apparent issues of singularities in early cosmology thanks to the nonlinearity parameter  $\beta$ .

Using Einstein's field equations and the energy-momentum tensor, the Ricci scalar curvature can be written as:

$$R = \rho_B - 3p_B. \quad (26)$$

In the same way, the Ricci tensor squared  $R_{\mu\nu}R^{\mu\nu}$  and the Kretschmann scalar  $R_{\mu\nu\alpha\beta}R^{\mu\nu\alpha\beta}$  can be expressed as: obtained as

$$R_{\mu\nu}R^{\mu\nu} = \rho_B^2 + 3p_B^2, \quad (27)$$

$$R_{\mu\nu\alpha\beta}R^{\mu\nu\alpha\beta} = \frac{5}{3}\rho_B^2 + 2\rho_B p_B + 3p_B^2. \quad (28)$$

Evidently, it is easy to see that the Ricci scalar curvature, the Ricci tensor and the Kretschmann scalar have no singularity at early/late stages,

$$\lim_{a(t) \rightarrow 0} R(t) = 4\rho_0, \quad (29)$$

$$\lim_{a(t) \rightarrow 0} R_{\mu\nu}R^{\mu\nu} = 4\rho_0^2, \quad (30)$$

$$\lim_{a(t) \rightarrow 0} R_{\mu\nu\alpha\beta}R^{\mu\nu\alpha\beta} = \frac{8\rho_0^2}{3}, \quad (31)$$

$$\lim_{a(t) \rightarrow \infty} R(t) = \lim_{a(t) \rightarrow \infty} R_{\mu\nu}R^{\mu\nu} = \lim_{a(t) \rightarrow \infty} R_{\mu\nu\alpha\beta}R^{\mu\nu\alpha\beta} = 0. \quad (32)$$

The absence of singularities at early/late is an attractive feature peculiar to NLED.

## B. Evolution

In this section, we will concentrate on the evolution of the EoS parameter  $\omega_B = p_B/\rho_B$ , the Hubble parameter  $H$  and the acceleration  $q$ .

The equation of state parameter is:

$$\omega_B = \frac{p_B}{\rho_B} = \frac{-1 + \frac{1}{3} \left( \frac{a}{a_{end}} \right)^{4\alpha}}{1 + \left( \frac{a}{a_I} \right)^{4\alpha}}. \quad (33)$$

It follows that for  $\alpha > 0$ ,

- at small scale  $a \ll a_{end}$

$$\omega_B = \frac{p_B}{\rho_B} \simeq -1 + \frac{4}{3} \left( \frac{a}{a_{end}} \right)^{4\alpha}, \quad (34)$$

- at large scale  $a \gg a_{end}$

$$\omega_B = \frac{p_B}{\rho_B} \simeq \frac{1}{3} - \frac{4}{3} \left( \frac{a_{end}}{a} \right)^{4\alpha}, \quad (35)$$

which shows that the Universe has a negative equation of state parameter for small  $a$  when the electromagnetic field is strong and radiation dominated Universe for large  $a$  when the field is weak.

The deceleration parameter is defined as follows:

$$q = -\frac{\ddot{a}a}{\dot{a}^2}. \quad (36)$$

Evidently, the Universe is decelerating when  $q > 0$  and accelerating when  $q < 0$ .

From Friedmann's equations, we get:

$$q = \frac{1}{2} (1 + 3\omega_B) = 1 - 2\beta\rho_B^\alpha. \quad (37)$$

It follows that,

- at small scale  $a \ll a_{end}$

$$q = -1 + 2 \left( \frac{a}{a_{end}} \right)^{4\alpha}, \quad (38)$$

- at large scale  $a \gg a_{end}$

$$q = 1 - 2 \left( \frac{a_{end}}{a} \right)^{4\alpha}. \quad (39)$$

Figure 1 shows the behavior of the equation of state parameter  $\omega_B$  and the deceleration  $q$  as function of the scale factor  $a$  for different values of  $\alpha = 0.1, 0.5, 1.5$ .

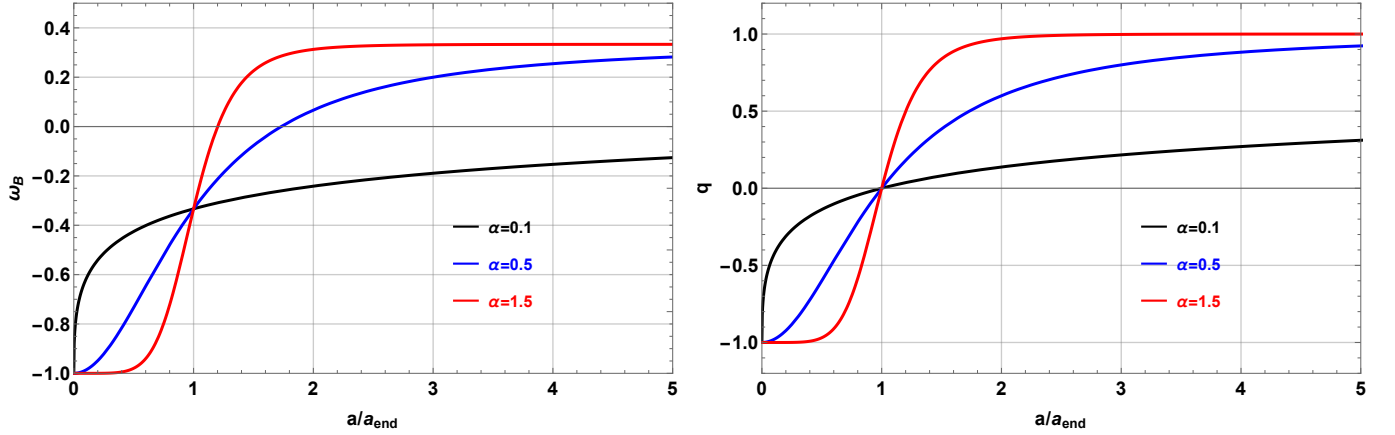


FIG. 1: EoS of state parameter  $\Omega_B$  and deceleration  $q$  as function of the scale factor  $a$  for different values of  $\alpha$ .

The first Friedmann equation gives the Hubble parameter as,

$$H^2 = \left( \frac{\dot{a}}{a} \right)^2 = \frac{\kappa^2}{3} \rho_B. \quad (40)$$

The above equation can be readily integrated yielding the following solution for the Hubble parameter,

$$t + const = \frac{1}{2H} {}_2F_1 \left( 1, -\frac{1}{2\alpha}; 1 - \frac{1}{2\alpha}; \frac{1}{2} \left( \frac{H}{H_{end}} \right)^{2\alpha} \right), \quad (41)$$

where  $H_{end} = H(a_{end})$  is the value of the Hubble parameter at the end of the inflation.

The evolution of the Hubble parameter with respect to the time is:

$$\dot{H} + 2H^2 \left( 1 - \frac{1}{2} \left( \frac{H}{H_{end}} \right)^{2\alpha} \right) = 0, \quad (42)$$

whose solution reads,

$$H = \frac{2^{\frac{1}{2\alpha}} H_{end}}{\left( 1 + \left( \frac{a}{a_{end}} \right)^{4\alpha} \right)^{1/2\alpha}}. \quad (43)$$

The square speed of sound is

$$c_s^2 = \frac{dp_B}{d\rho_B} = \frac{1 - (4\alpha + 3)\beta\mathcal{F}^\alpha}{3(\beta\mathcal{F}^\alpha + 1)}. \quad (44)$$

Asuming  $\beta\mathcal{F}^\alpha > 0$ , a requirement of classical stability and causality, i.e.  $0 < c_s^2 \leq 1$ , leads for

$$\left(\alpha < -\frac{3}{2} \wedge 0 \leq \beta\mathcal{F}^\alpha < -\frac{1}{2\alpha+3}\right) \vee \left(-\frac{3}{2} \leq \alpha \leq -\frac{3}{4} \wedge \beta\mathcal{F}^\alpha \geq 0\right) \vee \left(\alpha > -\frac{3}{4} \wedge 0 \leq \beta\mathcal{F}^\alpha < \frac{1}{4\alpha+3}\right). \quad (45)$$

Now, if we relax the condition  $\beta \geq 0$ , the region where a requirement of classical stability and causality holds is represented in Figure 2.

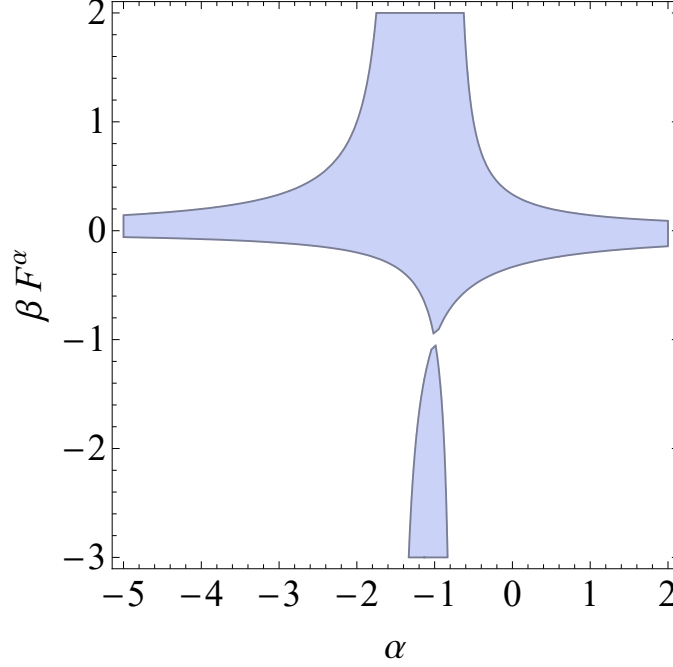


FIG. 2: Regions of parameter space  $\beta\mathcal{F}^\alpha$  vs.  $\alpha$  where a requirement of classical stability and causality is satisfied, i.e.  $0 < c_s^2 \leq 1$ .

### C. Cosmological Parameters

In this section, we will demonstrate that it is indeed possible to have a proper inflationary phase in the early Universe described by NLED coupled to Einstein gravity. To describe inflation, we use the e-folds number left to the end of inflation,

$$N = \ln\left(\frac{a_{end}}{a}\right). \quad (46)$$

Then,

$$\frac{dN}{dt} = -\frac{\dot{a}}{a} = -H. \quad (47)$$

In terms of e-folds number  $N$ , the energy density and the pressure read,

$$\begin{aligned} \rho(N) &= \frac{\rho_0}{(1 + e^{-4\alpha N})^{1/\alpha}} = \rho_{end} (1 + \tanh(2\alpha N))^{1/\alpha} \\ p(N) &= \rho(N) - f_1(N), \end{aligned} \quad (48)$$

where the function  $f_1(N)$  is given by:

$$f_1(N) = \frac{4}{3}\rho(1 - \beta\rho^\alpha).$$



The Hubble parameter will be:

$$\rho(N) = H_{end} (1 + \tanh(2\alpha N))^{\frac{1}{2\alpha}}. \quad (49)$$

In this formalism, the slow-roll parameters are defined as:

$$\begin{aligned} \epsilon &= \frac{d \ln H}{dN} \\ \eta &= \epsilon + \frac{1}{2} \frac{d \ln \epsilon}{dN}. \end{aligned} \quad (50)$$

where the first slow-roll parameter  $\epsilon$  is related to the measure of the acceleration during inflation, and the second slow-roll parameter  $\eta$  tells us how long the acceleration expression will be sustained.

The slow-roll parameters becomes,

$$\begin{aligned} \epsilon &= 1 - \tanh(2\alpha N) \\ \eta &= 1 - \alpha - (1 + \alpha) \tanh(2\alpha N). \end{aligned} \quad (51)$$

Therefore the tensor-to-scalar  $r$  and the scalar spectral index  $n_s$  can be expressed as:

$$\begin{aligned} r &= 16\epsilon = 16(1 - \tanh(2\alpha N)) \\ n_s &= -6\epsilon + 2\eta + 1 = -3 - 2\alpha + 2(2 - \alpha) \tanh(2\alpha N). \end{aligned} \quad (52)$$

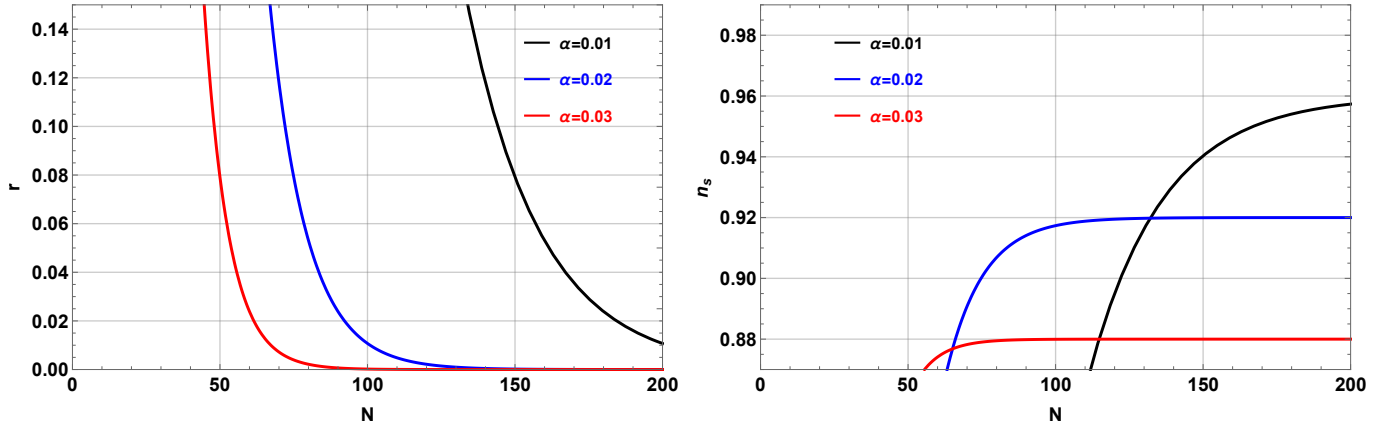


FIG. 3: The tensor-to-scalar  $r$  and the scalar spectral index  $n_s$  as function of the e-folds number  $N$  for different values of  $\alpha$ .

In figure 3, we plot the behavior of  $r$  and  $n_s$  as a function of the number of e-fold for different values of  $\alpha$ . The Planck 2018 bounds on the spectral index and the tensor-to-scalar ratio are the following,

$$n_s = 0.9649 \pm 0.0042, \quad r < 0.064. \quad (53)$$

It can be seen from the figures that the Planck 2018 result rules out the model. The figures show that the e-folding number must be large and  $\alpha$  extremely small to achieve successful inflation, away from the theoretical prior  $50 < N < 60$ .

To overcome the major drawback of the model given by (10), we propose the below generalized functional  $f(\mathcal{F})$  depending on three real parameters  $A$ ,  $\alpha$  and  $\beta$  as an alternative to the functional given by (10),

$$f(\mathcal{F}) = \frac{\mathcal{F}^{\frac{1}{4}(3A-1)}}{\left(1 + \beta \mathcal{F}^{\frac{3}{4}\alpha(A+1)}\right)^{1/\alpha}}. \quad (54)$$

It is clear that  $A = \frac{1}{3}$  reproduces the NLED model given by (10). The energy density of this model has the following e-folding number dependence,

$$\rho(N) = \rho_{end} \left( 1 + \tanh\left(\frac{3}{2}\alpha(A+1)N\right) \right)^{1/\alpha}, \quad (55)$$

where  $\rho_{end} = \frac{\rho_0}{2^{1/\alpha}} = \frac{1}{(2\beta)^{1/\alpha}}$ .

From the above equation, we obtain the the Hubble parameter as,

$$H(N) = H_{end} \left( 1 + \tanh \left( \frac{3}{2} \alpha (A+1) N \right) \right)^{1/2\alpha}. \quad (56)$$

One can now get the the scalar spectral index and the tensor-to-scalar as,

$$\begin{aligned} r &= 12(A+1) \left( 1 - \tanh \left( \frac{3}{2} \alpha (A+1) N \right) \right) \\ n_s &= 1 - \frac{3}{2}(A+1)(2+\alpha) + \frac{3}{2}(A+1)(2-\alpha) \tanh \left( \frac{3}{2} \alpha (A+1) N \right). \end{aligned} \quad (57)$$

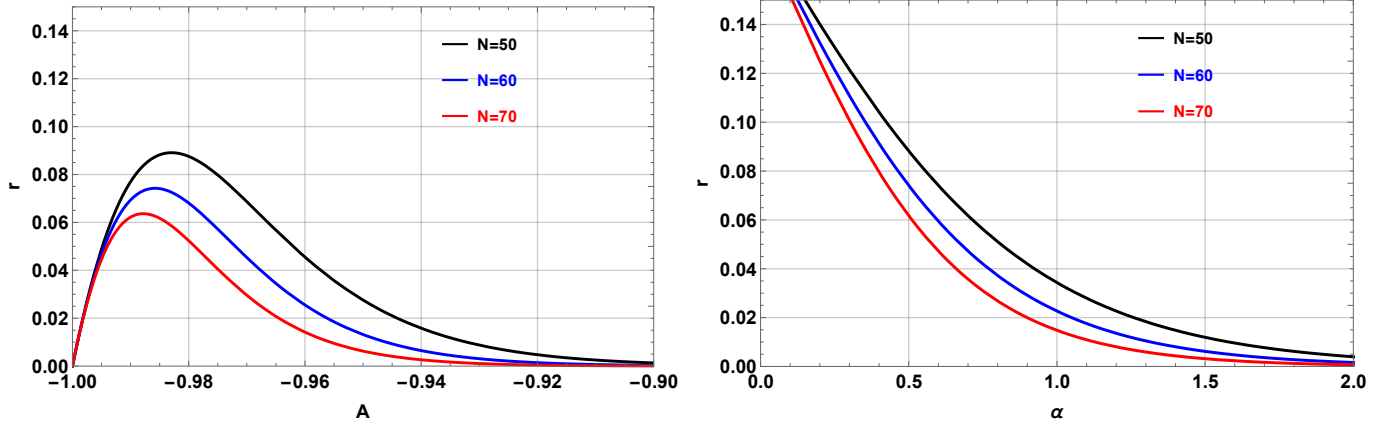


FIG. 4: The tensor-to-scalar ratio  $r$  as function of the parameter  $A$  with  $\alpha = 0.5$  and parameter  $\alpha$  with  $A = -0.985$  for  $N = 50, 60, 70$ .

Figure 4 displays the behavior of the tensor-to-scalar ratio  $r$  versus the parameter  $A$  by fixing  $\alpha = 0.5$  and the parameter  $\alpha$  by fixing  $A = -0.985$  for the e-folding number  $N = 50, 60$  and  $70$ . We note from the figure that the value of  $r$  increases till a maximum value and then decreases. We see that the bound  $r < 0.064$  is achieved for  $-1 < A < -0.995$  and  $-0.967 < A < 0$ . The figure indicates also that when  $\alpha$  increases the value of  $r$  decreases and the bound  $r < 0.064$  is satisfied for  $\alpha > 0.8$ .

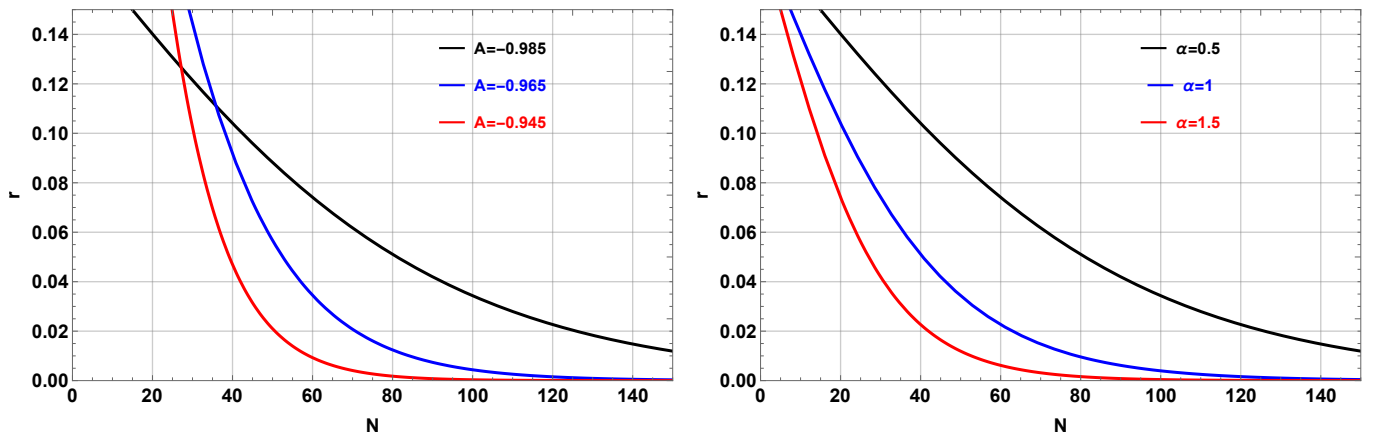


FIG. 5: The tensor-to-scalar ratio  $r$  as function of the e-fold number  $N$  for  $\alpha = 0.5$  with  $A = -0.985, -0.965, -0.945$  and for fixed  $A = -0.985$  with  $\alpha = 0.5, 1, 1.5$ .

In figure 5, we plot the tensor-to-scalar ratio  $r$  versus the e-folding number  $N$  for fixed  $\alpha = 0.5$  with  $A = -0.985, -0.965, -0.945$  and for fixed  $A = -0.985$  with  $\alpha = 0.5, 1, 1.5$ . The main observation from the

figure is that  $r$  decreases with the e-folding number.

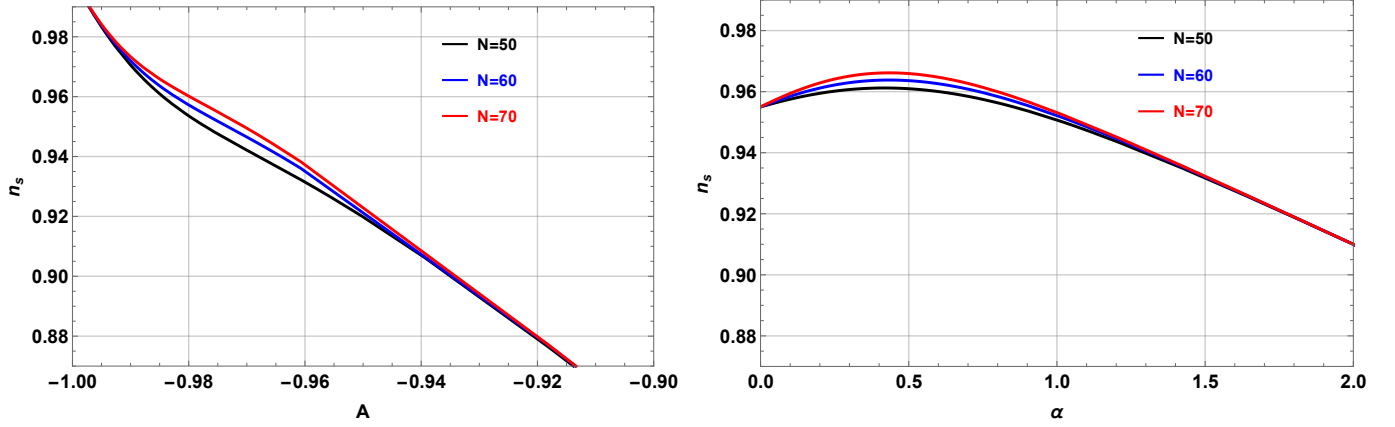


FIG. 6: The spectral index  $n_s$  as function of the parameter  $A$  with  $\alpha = 0.5$  and parameter  $\alpha$  with  $A = -0.985$  for  $N = 50, 60, 70$ .

Similarly, the figure 6 shows the variation of the spectral index  $n_s$  as a function of the parameter  $A$  by fixing  $\alpha = 0.5$  and the parameter  $\alpha$  by fixing  $A = -0.985$  for the e-folding number  $N$  equal to 50, 60 and 70. From the left figure in 6, the spectral index  $n_s$  decreases as the value of  $A$  increases whereas in the figure to the right, the spectral index  $n_s$  increases till a maximum and then decreases as  $\alpha$  increases.

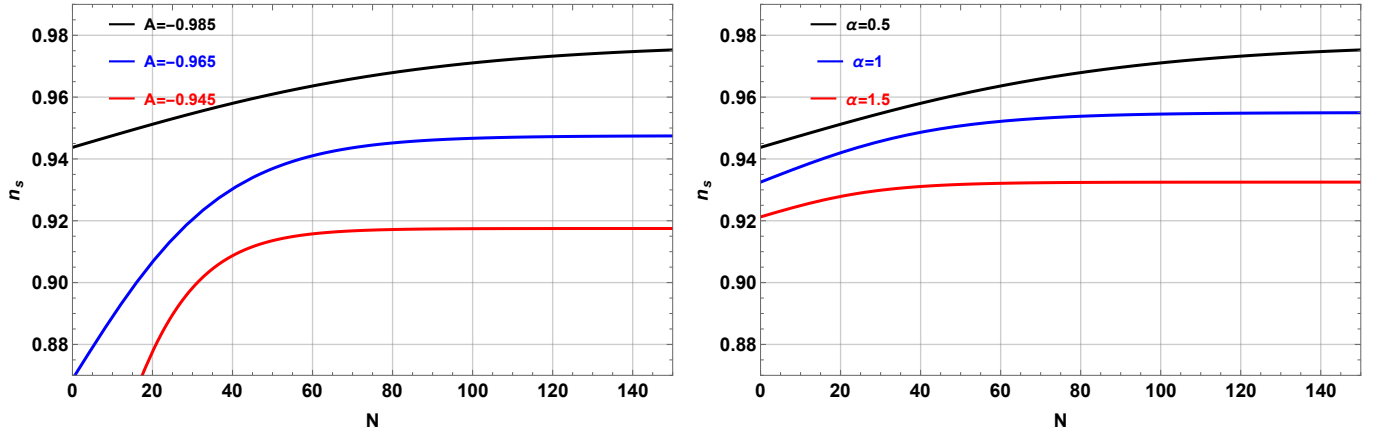


FIG. 7: The spectral index  $n_s$  as function of the e-fold number  $N$  for  $\alpha = 0.5$  with  $A = -0.985, -0.965, -0.945$  and for fixed  $A = -0.985$  with  $\alpha = 0.5, 1, 1.5$ .

In figure 7, we draw the spectral index  $n_s$  as a function of the e-folding number  $N$  for  $\alpha = 0.5$  with  $A = -0.985, -0.965, -0.945$  and for  $A = -0.985$  with  $\alpha = 0.5, 1, 1.5$ . In the figure to the left, for fixed value  $\alpha = 0.5$ , increasing  $A$  leads to lower values of the spectral index  $n_s$ . Additionally, similar tendency in the figure to the right is observe by fixing  $A = -0.985$  and increasing  $\alpha$ . Moreover, in order to present our results in a more transparent way, we plot in figure 8,  $r$  versus  $n_s$  by fixing  $\alpha = 0.5$  with  $-1 < A \leq -0.9$  and  $A = -0.985$  with  $0 < \alpha \leq 2$  for e-folding number  $N$  equal to 50, 60 and 70. It shows that the current bounds on  $n_s$  and  $r$  are satisfied.

#### D. A route to a generalization

Interestingly, one may use the Lagrangian (2) in such a way to describe all nonlinear electrodynamics models in the literature. While doing so, we want a unified prescription of all models. In the following, we provide an incomplete list of models that can be recovered from (2).

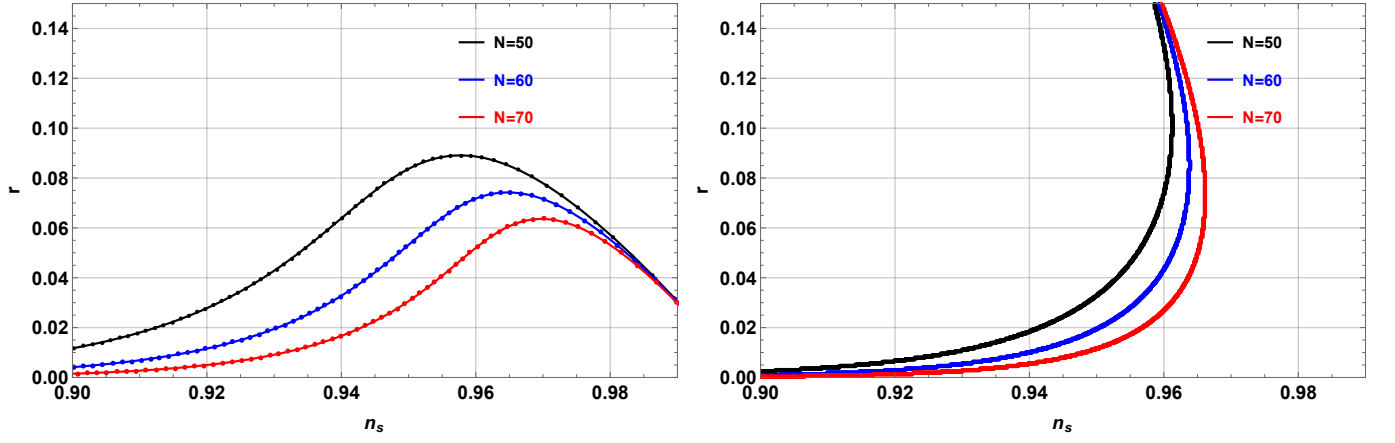


FIG. 8: The spectral index  $n_s$  as function of the tensor-to-scalar ratio  $r$  for  $\alpha = 0.5$  with  $A \in ]-1, -0.9]$  and for fixed  $A = -0.985$  with  $\alpha \in ]0, 2]$ .

Model	Lagrangian $\mathcal{L}$	$f(\mathcal{F})$	Maxwell's limit	References
Born-Infeld model	$-\alpha^2 \left( \sqrt{1 + \frac{2\mathcal{F}}{\alpha^2}} - 1 \right)$	$\frac{\alpha^2}{\mathcal{F}} \left( \sqrt{1 + \frac{2\mathcal{F}}{\alpha^2}} - 1 \right)$	$\alpha \gg \sqrt{2 \mathcal{F} }$	[70–72]
De Lorenci et al. model	$-\mathcal{F} + 16\alpha\mathcal{F}^2$	$1 - 16\alpha\mathcal{F}$	$\alpha \rightarrow 0$	[103]
Novello's Toy model	$-\mathcal{F} + 16\alpha^2\mathcal{F}^2 - \frac{\beta}{\mathcal{F}}$	$1 - 16\alpha\mathcal{F} + \frac{\beta}{\mathcal{F}^2}$	$\alpha \rightarrow 0, \beta \rightarrow 0$	[105]
Kruglov's model A	$-\mathcal{F} \left( 1 - \frac{\alpha}{2\beta\mathcal{F}+1} \right)$	$1 + \frac{1}{2\beta\mathcal{F}}$	$\alpha \rightarrow 0$	[104]
Kruglov's model B	$-\frac{\mathcal{F}}{\beta\mathcal{F}+1}$	$\frac{1}{\beta\mathcal{F}+1}$	$\beta \rightarrow 0$	[104]
Kruglov's model C	$-\mathcal{F} \text{sech}^2 \left( \sqrt[4]{ \mathcal{F}\beta } \right)$	$\text{sech}^2 \left( \sqrt[4]{ \mathcal{F}\beta } \right)$	$\beta\mathcal{F} \rightarrow 0$	[112]
Ovgun's exponential correction model	$\frac{-\mathcal{F}e^{-\alpha\mathcal{F}}}{\alpha\mathcal{F}+\beta}$	$\frac{e^{-\alpha\mathcal{F}}}{\alpha\mathcal{F}+\beta}$	$\alpha \rightarrow 0, \beta \rightarrow 0$	[109]
Benaoum and Övgün model	$\frac{-\mathcal{F}}{(\beta\mathcal{F}\alpha+1)^{1/\alpha}}$	$\frac{1}{(\beta\mathcal{F}\alpha+1)^{1/\alpha}}$	$\beta \rightarrow 0$	[113]

TABLE I: List of some NLED models.

The idea is to consider in the beginning that  $f = f(\mathcal{F})$  is an arbitrary functional. Then we proceed to specify some suitable conditions that the model at hand has to satisfy. From equation (9), the energy density, the pressure and the equation of state parameter for purely magnetic field (i.e.  $\vec{E} = \vec{0}$  and  $\mathcal{F} = \frac{1}{2}B^2$ ), we have

$$\rho_B = \mathcal{F}f, \quad p_B = \frac{1}{3}\mathcal{F}(f + 4\mathcal{F}f_{\mathcal{F}}), \quad \omega_B = \frac{p_B}{\rho_B} = \frac{1}{3} + \frac{4}{3}\mathcal{F}\frac{f_{\mathcal{F}}}{f}, \quad (58)$$

where we use the notations  $f_{\mathcal{F}} = f'(\mathcal{F})$ ,  $f_{\mathcal{F}\mathcal{F}} = f''(\mathcal{F})$ , ... The Ricci scalar which represents the curvature of the spacetime, calculated by using Einstein field equations and the energy momentum tensor,

$$R = \rho_B - 3p_B = -4\mathcal{F}^2 f_{\mathcal{F}}. \quad (59)$$

The Recci tensor squared  $R^{\mu\nu}R_{\mu\nu}$  and the Kretschmann  $R^{\mu\nu\alpha\beta}R_{\mu\nu\alpha\beta}$  are also obtained,

$$\begin{aligned} R^{\mu\nu}R_{\mu\nu} &= \rho_B^2 + 3p_B^2 = \frac{1}{3}\mathcal{F}^2 f^2 \left( 4 + 2\mathcal{F}\frac{f_{\mathcal{F}}}{f} + \mathcal{F}^2\frac{f_{\mathcal{F}}^2}{f^2} \right), \\ R^{\mu\nu\alpha\beta}R_{\mu\nu\alpha\beta} &= \frac{8}{3}\mathcal{F}^2 f^2 \left( 1 + 2\mathcal{F}\frac{f_{\mathcal{F}}}{f} + 2\mathcal{F}^2\frac{f_{\mathcal{F}}^2}{f^2} \right). \end{aligned} \quad (60)$$

The squared sound of speed is

$$c_s^2 = \frac{dp_B}{d\rho_B} = \frac{1}{3} + \frac{4}{3}\frac{2\mathcal{F}f_{\mathcal{F}} + \mathcal{F}^2 f_{\mathcal{F}\mathcal{F}}}{f + \mathcal{F}f_{\mathcal{F}}}. \quad (61)$$

In the following, we define the conditions that should satisfy viable NLfED:

1. Removal of singularities at early/late phase of the Universe. In flat spacetime, a sufficient condition for the Ricci scalar, the Ricci tensor squared, and the Kretschmann scalar to not be singular is to choose  $f = f(\mathcal{F})$  such that the energy density and the pressure are finite in the limit of large  $\mathcal{F}$  and small  $\mathcal{F}$ . Interestingly, in our approach, the pressure can be expressed in terms of the energy density and its derivative as:

$$p_B = \rho_B \left( -1 + \frac{4}{3} \frac{d\rho_B}{d\ln \mathcal{F}} \right). \quad (62)$$

This implies that in order to remove singularities to early/late phase of the Universe, both the energy  $\rho_B$  density and its derivative  $\frac{d\rho_B}{d\ln \mathcal{F}}$  have to be finite at  $a \rightarrow 0$  (large  $\mathcal{F}$ ) and  $a \rightarrow \infty$  (small  $\mathcal{F}$ ).

2. Early/late time radiation/dark energy domination phase for large/small magnetic field:

$$\lim_{\mathcal{F} \rightarrow \infty / \mathcal{F} \rightarrow 0} \frac{d\rho_B}{d\ln \mathcal{F}} = 1, 0 \implies \lim_{a \rightarrow 0 / a \rightarrow \infty} \omega_B = \frac{1}{3}, -1. \quad (63)$$

3. Condition of the accelerated Universe  $\rho_B + 3p_B < 0$  with the sources of NLfED fields are,

$$\begin{aligned} \rho_B + 3p_B &= \mathcal{F}f + \mathcal{F}(f + 4\mathcal{F}f_{\mathcal{F}}) \\ &= 2\rho_B \left( -1 + \frac{2}{3} \frac{d\ln \rho_B}{d\ln \mathcal{F}} \right). \end{aligned} \quad (64)$$

It gives,

$$\frac{\ln \rho_B}{d\ln \mathcal{F}} < \frac{3}{2}. \quad (65)$$

This inequality has to be satisfied for large  $B$ , that is, acceleration during the inflationary phase, and for small  $B$ , which corresponds to late-time acceleration.

4. Classical stability:

- (a) Causality of the Universe: the speed of the sound should be smaller than the local light speed ( $c_s < 1$ ) [93].
- (b) To avoid the Laplacian instability, we require the conditions that must be positive ( $c_s^2 > 0$ ).

The classical stability and causality give,

$$0 < \frac{1}{3} + \frac{4}{3} \frac{2\mathcal{F}f_{\mathcal{F}} + \mathcal{F}^2 f_{\mathcal{F}\mathcal{F}}}{f + \mathcal{F}f_{\mathcal{F}}} < 1, \quad (66)$$

which implies,

$$-\frac{1}{4} < \frac{d}{d\rho_B} (\mathcal{F}^2 f_{\mathcal{F}}) < \frac{1}{2}. \quad (67)$$

### E. Integrability and connection with the observables

In this section, we comment on the integrability of the system at hand. Moreover, we calculate some observables in the e-folding number  $N$ .

From the first equation of Friedmann's equations (14), one can obtain an equation which shows the conservation of energy for a particle moving in an effective potential  $V_{\text{eff}}(a)$ :

$$\frac{1}{2} \dot{a}^2 + V_{\text{eff}}(a) = 0, \quad (68)$$

with

$$V_{\text{eff}}(a) = -\frac{1}{6} a^2 \mathcal{F}f. \quad (69)$$

For a positive scale factor we get

$$\dot{a} = \frac{a}{\sqrt{3}} \sqrt{\mathcal{F}f}, \quad (70)$$

which can be solved by quadratures:

$$\frac{t}{\sqrt{3}} = \int \frac{1}{\sqrt{\mathcal{F}f}} dN. \quad (71)$$

For the generalized functional given by (54), we obtain,

$$t = -\frac{2}{(A+1)\sqrt{3}\rho_B} {}_2F_1\left(-\frac{1}{2\alpha}, -\frac{1}{2\alpha}; 1 - \frac{1}{2\alpha}; \frac{1}{2} \left(\frac{\rho_B}{\rho_{end}}\right)^\alpha\right) + C. \quad (72)$$

As a function of  $N := \ln(a_{end}/a)$ , the magnetic field  $B(N)$ , the magnetic field strength  $\mathcal{F}(N)$ , the Hubble parameter  $H(N)$  and the deceleration  $q(N)$  are (recall  $N = 0$  at the end of inflation):

$$\begin{aligned} B(N) &= B_{end} e^{2N}, \\ \mathcal{F}(N) &= \mathcal{F}_{end} e^{4N}, \\ H(N) &= \sqrt{\frac{1}{3} \mathcal{F}_{end} e^{4N} f(\mathcal{F}_{end} e^{4N})} = H_{end} e^{2N} \sqrt{\frac{f(\mathcal{F}_{end} e^{4N})}{f(\mathcal{F}_{end})}}, \\ q(N) &= -1 - \frac{\dot{H}}{H^2} = -1 + \frac{d \ln H}{dN} = 1 + \frac{2\mathcal{F}_{end} e^{4N} f'(\mathcal{F}_{end} e^{4N})}{f(\mathcal{F}_{end} e^{4N})}, \end{aligned} \quad (73)$$

where

$$H_{end} = \sqrt{\frac{1}{3} \mathcal{F}_{end} f(\mathcal{F}_{end})}. \quad (74)$$

Recall that at large scale  $a \gg a_{end}$ ,  $N < 0$ . The relation between  $N$  and the redshift is

$$N = \ln \left[ \frac{1+z}{1+z_{end}} \right]. \quad (75)$$

Then, we have

$$\begin{aligned} B(z) &= B_{end} \left[ \frac{1+z}{1+z_{end}} \right]^2, \\ \mathcal{F}(z) &= \mathcal{F}_{end} \left[ \frac{1+z}{1+z_{end}} \right]^4, \\ H(z) &= H_{end} \left[ \frac{1+z}{1+z_{end}} \right]^2 \sqrt{\frac{f\left(\mathcal{F}_{end} \left[\frac{1+z}{1+z_{end}}\right]^4\right)}{f(\mathcal{F}_{end})}}, \\ q(z) &= 1 + \frac{2\mathcal{F}_{end} \left[\frac{1+z}{1+z_{end}}\right]^4 f'\left(\mathcal{F}_{end} \left[\frac{1+z}{1+z_{end}}\right]^4\right)}{f\left(\mathcal{F}_{end} \left[\frac{1+z}{1+z_{end}}\right]^4\right)}. \end{aligned} \quad (76)$$

In figure 9, we illustrate the behavior of the EoS parameter  $\omega_B$  and deceleration  $q$  as function of the scale factor  $a$  for different values of  $\alpha$  and  $A = -0.985$ .

### III. PHASE SPACE ANALYSIS

In dynamical systems, phase space is a space in which all possible states of a system are represented. In phase space, every degree of freedom or parameter of the system is represented as an axis of a multidimensional space; a

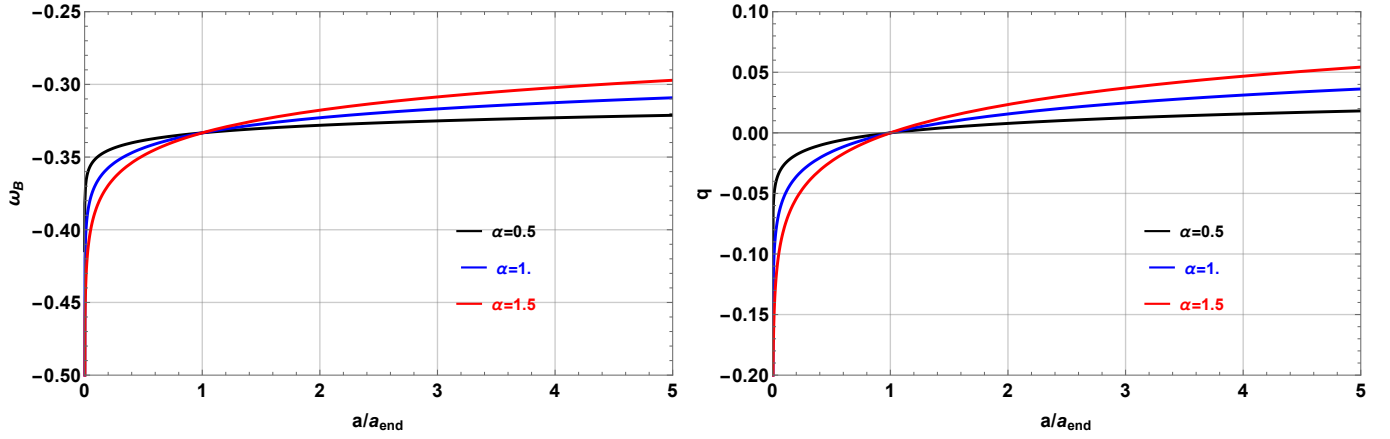


FIG. 9: EoS of state parameter  $\omega_B$  and deceleration  $q$  as function of the scale factor  $a$  for different values of  $\alpha$  and  $A = -0.985$ .

one-dimensional system is called a phase line, while a two-dimensional system is called a phase plane. Dynamical systems methods have been proved to be a powerful scheme for investigating the physical behaviour of cosmological models. As we know, there exist four standard ways of systematic investigation that can be used to examine cosmological models: (i) Obtaining and analyzing exact solutions; (ii) Heuristic approximation methods; (iii) Numerical simulation, and (iv) Qualitative analysis [124]. The last case can be used with three different approaches: (a) Piecewise approximation methods, (b) Hamiltonian methods, (c) Dynamical systems methods. In approach iv (a), the evolution of the model universe is approximated through a sequence of epochs in which specific terms in the governing differential equations can be neglected, leading to a more straightforward system of equations. This heuristic approach is firmly based on the existence of heteroclinic sequences, which is a concept from iv (c). In the approach iv (b), Einstein's equations are reduced to a Hamiltonian system dependent on time for a particle (point universe) in two dimensions. This approach has been used mainly for modelling and analyzing the dynamics of the Universe, nearly the Big-Bang singularity (this is one of the approaches we will follow). In the approach iv (c) Einstein's equations for homogeneous cosmologies can be described as an autonomous system of first-order ordinary differential equations plus certain algebraic constraints. Specifically, the Einstein's field equations of Bianchi's cosmologies and its isotropic subclass (FLRW models) can be written as an autonomous system of first-order differential equations whose solution curves partitioned to  $\mathbb{R}^n$  in orbits, defining a dynamical system in  $\mathbb{R}^n$ . In the general case, singular points, invariant sets, and other elements of the phase space partition can be listed and described. This study consists of several steps: determining singular points, the linearization in a neighbourhood of them, the search for the eigenvalues of the associated Jacobian matrix, checking the stability conditions in a neighbourhood of the singular points, the finding of the stability and instability sets and the determination of the basin of attraction, etcetera. On some occasions, to do that, it is needed to simplify a dynamic system. Two approaches are applied to this objective: one, reduce the dimensionality of the system, and two, eliminate the nonlinearity. Two rigorous mathematical techniques that allow substantial progress along both lines is the centre manifold theory and normal forms. Using this approach, in [124] many results have been obtained concerning the possible asymptotic cosmological states in Bianchi and FLRW models, whose material content is a perfect fluid (usually modelling "dark matter", a component that plays an important role in the formation of structures in the Universe, such as galaxies and clusters of galaxies) with linear equation of state (with the possible inclusion of a cosmological constant). Also, several classes of inhomogeneous models are examined, comparing the results with those obtained using numerical and Hamiltonian methods. This analysis is extended in [125], to other contexts, having considered other material sources such as the scalar fields.

Moreover, one can use tools of the theory of averaging in nonlinear differential equations, along with the qualitative analysis of dynamical systems, to obtain relevant information about the solution's space of cosmological models. The averaging methods were applied extensively in [126–131] to single field scalar field cosmologies, and for scalar field cosmologies with two scalar fields which interact only gravitationally with the matter in [132]. Whiting this context one deals with perturbation problems of differential systems which are expressed in Fenichel's normal form [133–139]. That is, given  $(x, y) \in \mathbb{R}^{n+m}$  and  $f, g$  smooth functions, equations can be written as:

$$\dot{x} = f(x, y; \varepsilon), \quad \dot{y} = \varepsilon g(x, y; \varepsilon), \quad x = x(t), \quad y = y(t). \quad (77)$$

The system (77) is called "fast system" as opposed to

$$\varepsilon x' = f(x, y; \varepsilon), \quad y' = g(x, y; \varepsilon), \quad x = x(\tau), \quad y = y(\tau), \quad (78)$$

which is obtained after the re scaling  $\tau = \varepsilon t$ , and is called “slow system”.

Notice that for  $\varepsilon > 0$ , the phase portraits of (77) and (78) coincide. It follows two problems that manifestly depend on two scales: (i) the problem in terms of the “slow time” variable, whose solution is analogous to the outer solution in a boundary layer problem; (ii) the fast system: a change of scale on the system which describes the rapid evolution that occurs in shorter times; analogous to the inner solution of a boundary layer problem. The solution of each subsystem will be sought in the form of a regular perturbation expansion. The subsystems will have simpler structures for singularly perturbed problems than the complete problems. Then, the slow and fast dynamics are characterized by reduced phase line or phase plane dynamics. Combining the results of these limit problems, information on the dynamics for small values of  $\varepsilon$  is obtained. This technique is used to construct uniformly valid approximations of the solutions of perturbation problems using seed solutions that satisfy the original equations in the limit of  $\varepsilon \rightarrow 0$  [137].

### A. Phase space analysis: pure NLED

The equation (68) represents the motion of a particle of the unit mass in the effective potential. This equation is satisfied on the zero-energy level, where  $\rho_B$  plays the role of effective energy density parameterized through the scale factor  $a(t)$ . Therefore the standard cosmological model can be represented in terms of a dynamical system of a Newtonian type:

$$\ddot{a} = -\frac{\partial V_{\text{eff}}}{\partial a}, \quad V_{\text{eff}}(a) = -\frac{\mathcal{F}_{\text{end}} a_{\text{end}}^4}{6a^2} f\left(\mathcal{F}_{\text{end}} \left(\frac{a_{\text{end}}}{a}\right)^4\right), \quad (79)$$

where the scale factor  $a$  plays the role of a positional variable of a fictitious particle of the unit mass, which mimics the expansion of the Universe.

We assume  $\mathcal{F}_{\text{end}} > 0$ , and introduce the variables

$$\frac{a}{a_{\text{end}}} = e^u = e^{-N}, \quad v = \frac{\dot{a}}{a_{\text{end}}} \frac{1}{\sqrt{2\mathcal{F}_{\text{end}}}}, \quad (80)$$

and the time variable

$$\tau = \sqrt{2\mathcal{F}_{\text{end}}} \int e^{-u} dt. \quad (81)$$

This system can be written in the form

$$\frac{du}{d\tau} = v, \quad \frac{dv}{d\tau} = -\frac{\partial W(u)}{\partial u}, \quad (82)$$

with effective particle-potential

$$W(u) = -\frac{1}{12} e^{-2u} f(\mathcal{F}_{\text{end}} e^{-4u}). \quad (83)$$

Thus,  $\frac{v^2}{2} + W(u) = E$ , is the constant of energy. From the above system we see that, generically, the equilibrium points of the system (82) are situated on the axis  $u$  ( $v = 0$ ) and they satisfy  $\frac{\partial W(u)}{\partial u} = 0$ . From the characteristic equation it follows that just three types of equilibrium points are admitted:

1. Saddle if  $u_c : \frac{\partial W}{\partial u}|_{u=u_c} = 0$  and  $\frac{\partial^2 W}{\partial u^2}|_{u=u_c} < 0$ ;
2. Focus if  $u_c : \frac{\partial W}{\partial u}|_{u=u_c} = 0$  and  $\frac{\partial^2 W}{\partial u^2}|_{u=u_c} > 0$ ;
3. Degenerated critical point if  $u_c : \frac{\partial W}{\partial u}|_{u=u_c} = 0$  and  $\frac{\partial^2 W}{\partial u^2}|_{u=u_c} = 0$ .

We have the expressions

$$\begin{aligned} W'(u) &= \frac{1}{3} \mathcal{F}_{\text{end}} e^{-6u} f'(\mathcal{F}_{\text{end}} e^{-4u}) + \frac{1}{6} e^{-2u} f(\mathcal{F}_{\text{end}} e^{-4u}) \\ W''(u) &= -\frac{4}{3} \mathcal{F}_{\text{end}}^2 e^{-10u} f''(\mathcal{F}_{\text{end}} e^{-4u}) - \frac{8}{3} \mathcal{F}_{\text{end}} e^{-6u} f'(\mathcal{F}_{\text{end}} e^{-4u}) - \frac{1}{3} e^{-2u} f(\mathcal{F}_{\text{end}} e^{-4u}). \end{aligned} \quad (84)$$



The eigenvalues of the Jacobian matrix evaluated at the equilibrium point with coordinate  $u_c$  are  $\left\{-i\sqrt{W'''(u_c)}, i\sqrt{W'''(u_c)}\right\}$ , such that the condition for having periodic solutions is  $W''(u_c) > 0$ . Since  $W'(u_c) = 0$  at the equilibrium points we end up with the condition  $2\mathcal{F}_{end} f''(\mathcal{F}_{end} e^{-4u_c}) + 3e^{4u_c} f'(\mathcal{F}_{end} e^{-4u_c}) < 0$  as a sufficient condition for having a cyclic Universe.

Due to the relation  $\mathcal{F} = \mathcal{F}_{end} e^{-4u}$ , the above conditions can be summarized as follows:

1. The equilibrium points are given by  $u_c = 1/4 \ln(\mathcal{F}_{end}/\mathcal{F}_c)$ , where

$$2\mathcal{F}_c f'(\mathcal{F}_c) + f(\mathcal{F}_c) = 0. \quad (85)$$

The above equation must be considered an algebraic (in most cases transcendent) equation of  $\mathcal{F}_c$  for a given  $f$  and not a differential equation for  $f$ .

Furthermore, evaluated at the equilibrium point we obtain  $\rho_B + 3p_B = 0$ . That is zero acceleration point. This is not unexpected since the condition for obtaining the equilibrium points is  $\ddot{a} = 0$ . Evaluating at the equilibrium point, we obtain  $c_s^2|_{u=u_c} = -\frac{4}{3} \frac{f''(\mathcal{F}_c)}{f'(\mathcal{F}_c)} - \frac{7}{3}$ . The conditions for classical stability at the equilibrium points will be

$$\frac{7}{4} \leq -\frac{f''(\mathcal{F}_c)}{f'(\mathcal{F}_c)} < \frac{5}{2}. \quad (86)$$

2. The equilibrium point is a saddle for

$$4\mathcal{F}_c^2 f''(\mathcal{F}_c) + 8\mathcal{F}_c f'(\mathcal{F}_c) + f(\mathcal{F}_c) > 0, \quad (87)$$

or, equivalently:

$$2\mathcal{F}_{end}^2 f''(\mathcal{F}_c) + 3\mathcal{F}_c f'(\mathcal{F}_c) > 0. \quad (88)$$

3. The equilibrium point is a focus for

$$\frac{\partial^2 W}{\partial u^2} \Big|_{u=u_c} > 0$$

or, equivalently:

$$2\mathcal{F}_{end}^2 f''(\mathcal{F}_c) + 3\mathcal{F}_c f'(\mathcal{F}_c) < 0. \quad (89)$$

This condition leads to the existence of periodic solutions.

4. It is degenerate for

$$f'(\mathcal{F}_c) = -\frac{f(\mathcal{F}_c)}{2\mathcal{F}_c}, \quad f''(\mathcal{F}_c) = \frac{3f(\mathcal{F}_c)}{4\mathcal{F}_c^2}. \quad (90)$$

Using (54), the effective potential is written as

$$W(u) = -\frac{1}{12} \mathcal{F}_{end}^{\frac{3A}{4}-\frac{1}{4}} e^{-(3A+1)u} \left( \beta \mathcal{F}_{end}^{\frac{3}{4}\alpha(A+1)} e^{-3\alpha(A+1)u} + 1 \right)^{-1/\alpha}. \quad (91)$$

System (82) becomes

$$\frac{du}{d\tau} = v, \quad (92)$$

$$\frac{dv}{d\tau} = \frac{1}{12} \mathcal{F}_{end}^{\frac{1}{4}(3A-1)} e^{-u(3\alpha+3(\alpha+1)A+1)} \left( 2\beta \mathcal{F}_{end}^{\frac{3}{4}\alpha(A+1)} - (3A+1)e^{3\alpha(A+1)u} \right) \left( \beta \mathcal{F}_{end}^{\frac{3}{4}\alpha(A+1)} e^{-3\alpha(A+1)u} + 1 \right)^{-\frac{1}{\alpha}-1}. \quad (93)$$

The equilibrium points of system (82) are  $(u_c, 0)$  such that  $u_c = 1/4 \ln(\mathcal{F}_{end}/\mathcal{F}_c)$  where  $\mathcal{F}_c$  are the roots of (85) which is reduced to

$$\mathcal{F}_c^{\frac{1}{4}(3A+1)} \left( 2\beta \mathcal{F}_c^{\frac{3}{4}\alpha(A+1)} - 3A - 1 \right) \left( \beta \mathcal{F}_c^{\frac{3}{4}\alpha(A+1)} + 1 \right)^{-\frac{\alpha+1}{\alpha}} = 0. \quad (94)$$

We assume  $\mathcal{F}_c \neq 0$ , then, we have either  $\mathcal{F}_c^{\frac{3}{4}\alpha(A+1)} = \beta^{-1}(1+3A)/2$  (for all values of  $\alpha$  and  $(1+3A)/\beta > 0$ ) or  $\mathcal{F}_c^{\frac{3}{4}\alpha(A+1)} = -\beta^{-1}$  (provided  $-1 < \alpha < 0, \beta < 0$ ). That is,  $\mathcal{F}_c = [\beta^{-1}(1+3A)/2]^{\frac{4}{3\alpha(A+1)}}$  (for all values of  $\alpha$  and  $(1+3A)/\beta > 0$ ) or  $\mathcal{F}_c = (-\beta)^{-\frac{4}{3\alpha(A+1)}}$  (provided  $-1 < \alpha < 0, \beta < 0$ ). Hence, the equilibrium points are

$$P_0 := \left( \frac{\ln(2)}{3\alpha(1+A)} + \frac{1}{4} \ln \left[ \mathcal{F}_{end} \left( \frac{3A+1}{\beta} \right)^{-\frac{4}{3\alpha(1+A)}} \right], 0 \right), \quad P_1 := \left( \frac{1}{4} \left( \ln(\mathcal{F}_{end}) - \frac{4 \ln \left[ -\frac{1}{\beta} \right]}{3\alpha(A+1)} \right), 0 \right). \quad (95)$$

$P_0$  exists for  $(1+3A)/\beta > 0$  and  $P_1$  exists for  $-1 < \alpha < 0, \beta < 0$ . From physical conditions we assume  $\beta \geq 0$ . That is, the equilibrium point  $P_1$  is discarded. Then, for  $P_0$  does exists we require  $A > -1/3, \beta > 0$ .

The linearization matrix evaluated at  $P_0$  has eigenvalues

$$\begin{aligned} & -\frac{i3^{-\frac{\alpha+1}{2\alpha}} \sqrt{\alpha} 2^{\frac{1}{3\alpha+3\alpha A}-\frac{1}{2}} (A+1)^{-\frac{1}{2\alpha}} (3A+1)^{\frac{1}{6}(\frac{3A+1}{\alpha+\alpha A}+3)} \beta^{-\frac{3A+1}{6\alpha+6\alpha A}}}{\sqrt[4]{\mathcal{F}_{end}}}, \\ & \frac{i3^{-\frac{\alpha+1}{2\alpha}} \sqrt{\alpha} 2^{\frac{1}{3\alpha+3\alpha A}-\frac{1}{2}} (A+1)^{-\frac{1}{2\alpha}} (3A+1)^{\frac{1}{6}(\frac{3A+1}{\alpha+\alpha A}+3)} \beta^{-\frac{3A+1}{6\alpha+6\alpha A}}}{\sqrt[4]{\mathcal{F}_{end}}}. \end{aligned}$$

For  $\alpha < 0, A > -1/3, \beta > 0$  the eigenvalues are reals and of different signs. Then  $P_0$  is a saddle. If  $\alpha > 0, A > -1/3, \beta > 0$  the eigenvalues are purely imaginary, and the point is nonhyperbolic.

On the other hand, using the generating function  $f$  given by is (54), condition for classical stability and causality is (86) for  $P_0$  is

$$\frac{7}{4} \leq -2^{\frac{4}{3\alpha+3\alpha A}-2} (3A+1)^{-\frac{4}{3\alpha+3\alpha A}} (\alpha+3\alpha A-6) \beta^{\frac{4}{3\alpha+3\alpha A}} < \frac{5}{2}. \quad (96)$$

Then, assuming  $\alpha > 0, A > -1/3, \beta > 0$ , we have that  $P_0$  can be a nonlinear centre or nonlinear spiral (because it is nonhyperbolic), and additionally, the condition for classical stability and causality is given by (96). Due to the non-hyperbolicity, we use numerical methods to investigate the stability.

For the numerics it is convenient to use the variables  $(\mathcal{F}, v)$  through the redefinition  $u = 1/4 \ln(\mathcal{F}_{end}/\mathcal{F})$ . Hence,

$$\frac{d\mathcal{F}}{d\tau} = -4v\mathcal{F}, \quad (97)$$

$$\frac{dv}{d\tau} = \varepsilon \left\{ \mathcal{F}^{\frac{1}{4}(3A+1)} \left( \beta \mathcal{F}^{\frac{3}{4}\alpha(A+1)} + 1 \right)^{-\frac{\alpha+1}{\alpha}} \left( 2\beta \mathcal{F}^{\frac{3}{4}\alpha(A+1)} - 3A - 1 \right) \right\}, \quad (98)$$

where

$$\varepsilon := \frac{1}{12\sqrt{\mathcal{F}_{end}}}. \quad (99)$$

For the analysis of system (97) and (98) we consider the parameter values  $\alpha \in \{0.5, 1.0, 1.5\}$  with  $A \in \{-0.985, -0.965, -0.945\}$  and  $\beta = 1$ . Moreover, according to our previous estimations, for the theoretical prior  $z_{end} \simeq 10^{-2} z_{GUT}$ , we have  $5 \times 10^{23} \text{cm}^{-2} \lesssim \mathcal{F}_{end} \lesssim 5 \times 10^{37} \text{cm}^{-2}$ . Then, we have  $1.17851 \times 10^{-20} \text{cm} \lesssim \varepsilon := \frac{1}{12\sqrt{\mathcal{F}_{end}}} \lesssim 1.17851 \times 10^{-13} \text{cm}$ , therefore, we are in presence of a fast-slow system. The system (97) and (98) gives the dynamics in the fast manifold. That corresponds to the “horizontal motion”  $v = v_0$  (constant), and

$$\frac{d\mathcal{F}}{d\tau} = -4v_0\mathcal{F} \implies \mathcal{F}(\tau) = \mathcal{F}(\tau_0) e^{-4v_0(\tau-\tau_0)}. \quad (100)$$

This fact is confirmed numerically, by considering the parameter region

$$\alpha \in \{0.5, 1., 1.5\}, A \in \{-0.985, -0.965, -0.945\}, \mathcal{F}_{end} \in \{5 \times 10^{23}, 5 \times 10^{37}\}, \beta = 1. \quad (101)$$

In figure 10 is presented the horizontal flow of the system (97) and (98) for some values in the parameter space (101) and  $\mathcal{F}_{end} = 5 \times 10^{23}$ . Moreover, in figure 11 is presented the horizontal flow of the system (97) and (98) for some values in the parameter space (101) and  $\mathcal{F}_{end} = 5 \times 10^{37}$ .

Using the slow time  $T = \varepsilon\tau$ , we have the system

$$\varepsilon \frac{d\mathcal{F}}{dT} = -4v\mathcal{F}, \quad (102)$$

$$\frac{dv}{dT} = \mathcal{F}^{\frac{1}{4}(3A+1)} \left( \beta \mathcal{F}^{\frac{3}{4}\alpha(A+1)} + 1 \right)^{-\frac{\alpha+1}{\alpha}} \left( 2\beta \mathcal{F}^{\frac{3}{4}\alpha(A+1)} - 3A - 1 \right). \quad (103)$$

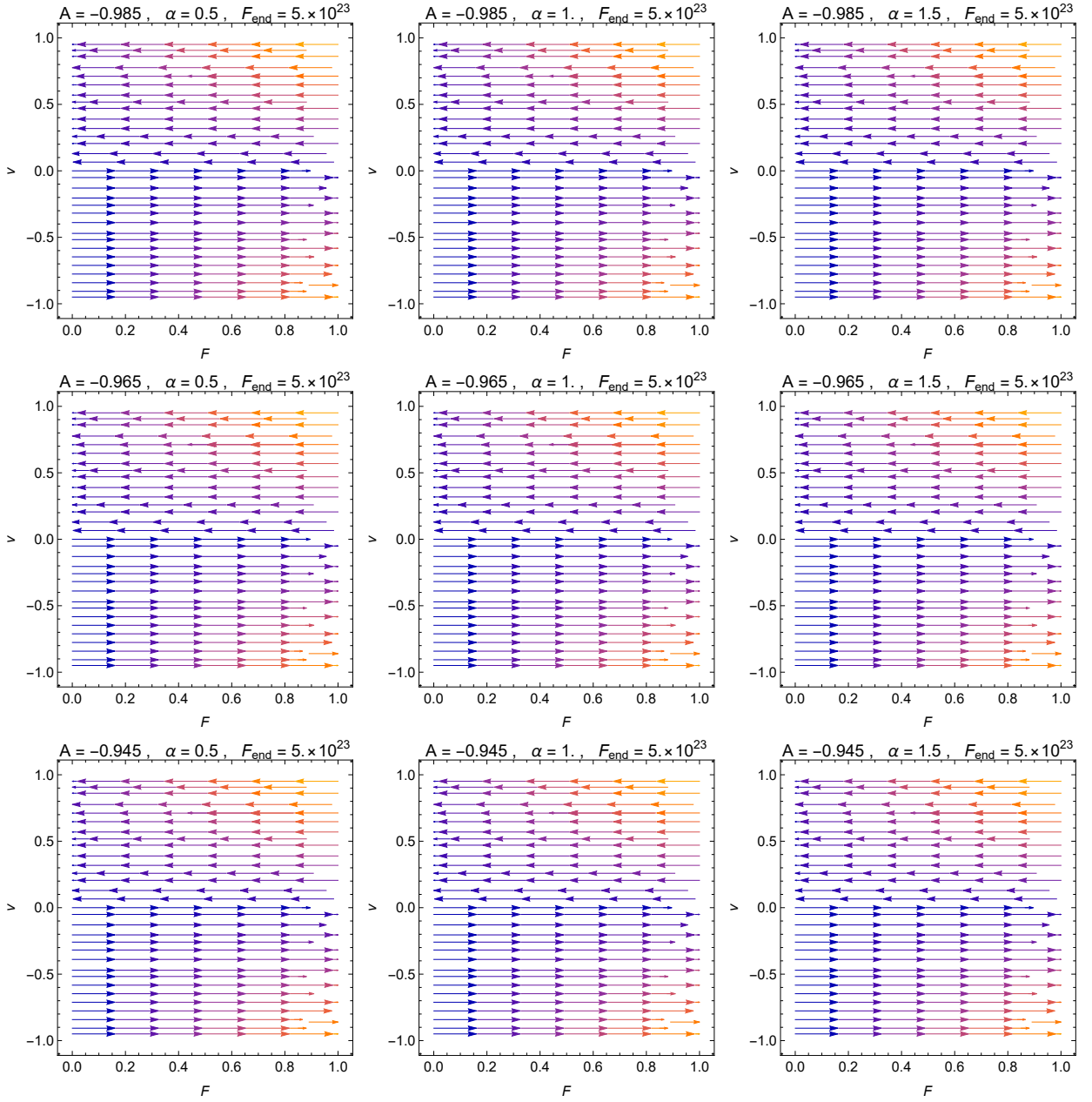


FIG. 10: Horizontal flow of the system (97) and (98) for some values in the parameter space (101) and  $\mathcal{F}_{end} = 5 \times 10^{23}$

We can easily see that the dynamics at the slow manifold is governed by the equilibrium points  $(\mathcal{F}, v)$  which satisfies  $v = 0$  and  $\left(\beta\mathcal{F}^{\frac{3}{4}\alpha(A+1)} + 1\right)^{-\frac{\alpha+1}{\alpha}} \left(2\beta\mathcal{F}^{\frac{3}{4}\alpha(A+1)} - 3A - 1\right) = 0$ . That is, depending on the parameter values, the attractors are  $P_0$  or  $P_1$ . They were analyzed before in the coordinates  $(u, v)$ . Notice that the axis  $(\mathcal{F}, v) = (0, v_c)$  is a line of equilibrium points, with eigenvalues  $\{0, -4v_c\}$ .

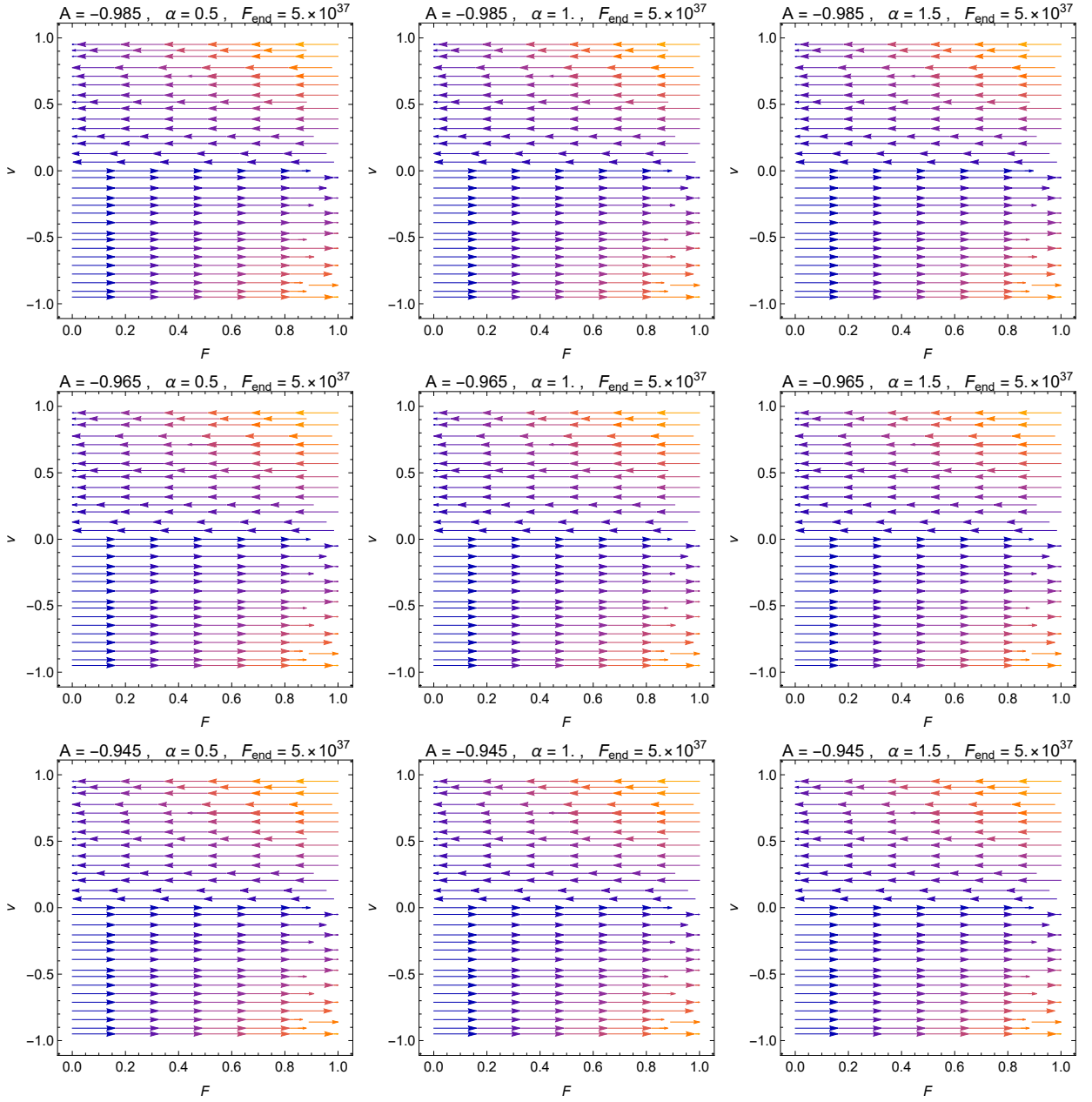


FIG. 11: Horizontal flow of the system (97) and (98) for some values in the parameter space (101) and  $\mathcal{F}_{end} = 5 \times 10^{37}$

### B. Phase space analysis: NLED including matter

For the metric (13), the Friedmann equations for NLED with an extra matter source (a matter fluid with density  $\rho_m$ , pressure  $p_m$  and a barotropic equation of state  $p_m = w_m \rho_m$ ) can be easily computed which results in,

$$\begin{aligned} H^2 &= \left( \frac{\dot{a}}{a} \right)^2 = \frac{1}{3} (\rho_B + \rho_m), \\ 3 \frac{\ddot{a}}{a} &= -\frac{1}{2} (\rho_B + 3p_B + \rho_m + 3p_m), \end{aligned} \quad (104)$$

where  $H = \dot{a}/a$  is the Hubble parameter.

Using the conservation of the energy-momentum tensor  $\nabla^\mu T_{\mu\nu} = 0$ , the continuity equation of the NLED is given

by (15). The continuity equation for barotropic matter is given by

$$\dot{\rho}_m + 3(1 + w_m)H\rho_m = 0. \quad (105)$$

Therefore,

$$\rho_m = \rho_{m,end} \left( \frac{a_{end}}{a} \right)^{3(1+w_m)} = \rho_{m,end} \left( \frac{1+z}{1+z_{end}} \right)^{3(1+w_m)}. \quad (106)$$

where

$$\rho_{m,end} = 3H_{end}^2 - \rho_{end}, \quad \rho_{end} = \mathcal{F}_{end} f(\mathcal{F}_{end}). \quad (107)$$

We have

$$q(z) = -1 + \frac{(1+z)}{2} \frac{d \ln H^2(z)}{dz}, \quad (108)$$

where

$$H^2(z) = \frac{1}{3} \left\{ \mathcal{F}_{end} \left( \frac{1+z}{1+z_{end}} \right)^4 f \left( \mathcal{F}_{end} \left[ \frac{1+z}{1+z_{end}} \right]^4 \right) + (3H_{end}^2 - \mathcal{F}_{end} f(\mathcal{F}_{end})) \left( \frac{1+z}{1+z_{end}} \right)^{3(1+w_m)} \right\}. \quad (109)$$

We assume  $\mathcal{F}_{end} > 0$ , and using the variables (80), and the time variable  $\tau$  given by (81), the system is then equivalent to

$$\frac{du}{d\tau} = v, \quad \frac{dv}{d\tau} = -\frac{\partial W(u)}{\partial u}, \quad (110)$$

where the effective potential is

$$W(u) = -\frac{1}{12} \frac{\rho_{m,end}}{\mathcal{F}_{end}} e^{-u(3w_m+1)} - \frac{1}{12} e^{-2u} f(\mathcal{F}_{end} e^{-4u}). \quad (111)$$

Now, the equilibrium points are found by solving numerically

$$W'(u) = 0. \quad (112)$$

As in the previous section, a given equilibrium point  $u_c$  is of one the following types:

1. saddle if  $u_c : \frac{\partial W}{\partial u}|_{u=u_c} = 0$  and  $\frac{\partial^2 W}{\partial u^2}|_{u=u_c} < 0$ ;
2. focus if  $u_c : \frac{\partial W}{\partial u}|_{u=u_c} = 0$  and  $\frac{\partial^2 W}{\partial u^2}|_{u=u_c} > 0$ ;
3. degenerated critical point if  $u_c : \frac{\partial W}{\partial u}|_{u=u_c} = 0$  and  $\frac{\partial^2 W}{\partial u^2}|_{u=u_c} = 0$ .

We have the expressions

$$W'(u) = \frac{1}{3} \mathcal{F}_{end} e^{-6u} f'(\mathcal{F}_{end} e^{-4u}) + \frac{1}{6} e^{-2u} f(\mathcal{F}_{end} e^{-4u}) + \frac{\rho_{m,end}(3w_m+1)e^{-u(3w_m+1)}}{12\mathcal{F}_{end}}, \quad (113)$$

$$W''(u) = -\frac{4}{3} \mathcal{F}_{end} e^{-10u} (\mathcal{F}_{end} f''(\mathcal{F}_{end} e^{-4u}) + 2e^{4u} f'(\mathcal{F}_{end} e^{-4u})) - \frac{1}{3} e^{-2u} f(\mathcal{F}_{end} e^{-4u}) - \frac{\rho_{m,end}(3w_m+1)^2 e^{-u(3w_m+1)}}{12\mathcal{F}_{end}}. \quad (114)$$

As before the eigenvalues of the Jacobian matrix evaluated at the equilibrium point with coordinate  $u_c$  are  $\{-i\sqrt{W''(u_c)}, i\sqrt{W''(u_c)}\}$ , such that the condition for having periodic solutions is  $W''(u_c) > 0$ . Since  $W'(u_c) = 0$  at

the equilibrium points,  $u_c$  satisfies the equation  $\frac{2\mathcal{F}_{end}e^{u_c(3w_m-5)}(2\mathcal{F}_{end}f'(\mathcal{F}_{end}e^{-4u_c})+e^{4u_c}f(\mathcal{F}_{end}e^{-4u_c}))}{3w_m+1} + \rho_{m,end} = 0$ ,

we end up with the condition

$$2\mathcal{F}_{end}e^{2u_c}(e^{4u_c}(3w_m-7)f'(\mathcal{F}_{end}e^{-4u_c}) - 4\mathcal{F}_{end}f''(\mathcal{F}_{end}e^{-4u_c})) + e^{10u_c}(3w_m-1)f(\mathcal{F}_{end}e^{-4u_c}) > 0$$

as a sufficient condition for having a cyclic universe.

Due to the relation  $\mathcal{F} = \mathcal{F}_{end}e^{-4u}$ , the above conditions can be summarized as follows:

1. The equilibrium points are given by  $u_c = 1/4 \ln(\mathcal{F}_{end}/\mathcal{F}_c)$ , where  $\mathcal{F}_c$  are the zeroes of the algebraic (most of the cases transcendent) equation

$$2\mathcal{F}_c (2\mathcal{F}_c f'(\mathcal{F}_c) + f(\mathcal{F}_c)) + (3w_m + 1)\rho_{m,end} \left( \frac{\mathcal{F}_c}{\mathcal{F}_{end}} \right)^{\frac{3(w_m+1)}{4}} = 0, \quad (115)$$

for a given  $f$ .

2. The equilibrium point is a saddle for

$$(2\mathcal{F}_c (4\mathcal{F}_c f''(\mathcal{F}_c) + (7 - 3w_m)f'(\mathcal{F}_c)) + (1 - 3w_m)f(\mathcal{F}_c)) > 0. \quad (116)$$

3. The equilibrium point is a focus for

$$(2\mathcal{F}_c (4\mathcal{F}_c f''(\mathcal{F}_c) + (7 - 3w_m)f'(\mathcal{F}_c)) + (1 - 3w_m)f(\mathcal{F}_c)) < 0. \quad (117)$$

This condition leads to the existence of periodic solutions.

4. It is degenerated for

$$f'(\mathcal{F}_c) = -\frac{2\mathcal{F}_c f(\mathcal{F}_c) + \rho_{m,end}(1 + 3w_m) \left( \frac{\mathcal{F}_{end}}{\mathcal{F}_c} \right)^{-\frac{3}{4}(w_m+1)}}{4\mathcal{F}_c^2}, \quad (118)$$

$$f''(\mathcal{F}_c) = \frac{12\mathcal{F}_c f(\mathcal{F}_c) + \rho_{end}(7 - 9(w_m - 2)w_m) \left( \frac{\mathcal{F}_{end}}{\mathcal{F}_c} \right)^{-\frac{3}{4}(w_m+1)}}{16\mathcal{F}_c^3}. \quad (119)$$

We apply the procedure to the present model (54). That is, using (54), the effective potential is written as

$$W(u) = -\frac{1}{12} \frac{\rho_{m,end}}{\mathcal{F}_{end}} e^{-u(3w_m+1)} - \frac{1}{12} \mathcal{F}_{end}^{\frac{3A}{4}-\frac{1}{4}} e^{-(3A+1)u} \left( \beta \mathcal{F}_{end}^{\frac{3}{4}\alpha(A+1)} e^{-3\alpha(A+1)u} + 1 \right)^{-1/\alpha}. \quad (120)$$

System (82) becomes

$$\frac{du}{d\tau} = v, \quad (121)$$

$$\begin{aligned} \frac{dv}{d\tau} = & -\frac{\rho_{m,end}(3w_m + 1)e^{-u(3w_m+1)}}{12\mathcal{F}_{end}} \\ & + \frac{1}{12} \mathcal{F}_{end}^{\frac{1}{4}(3A-1)} e^{-u(3\alpha+3(\alpha+1)A+1)} \left( 2\beta \mathcal{F}_{end}^{\frac{3}{4}\alpha(A+1)} - (3A+1)e^{3\alpha(A+1)u} \right) \left( \beta \mathcal{F}_{end}^{\frac{3}{4}\alpha(A+1)} e^{-3\alpha(A+1)u} + 1 \right)^{-\frac{1}{\alpha}-1}. \end{aligned} \quad (122)$$

For the numerics it is convenient to use the variables  $(\mathcal{F}, v)$  through the redefinition  $u = 1/4 \ln(\mathcal{F}_{end}/\mathcal{F})$ . Hence,

$$\frac{d\mathcal{F}}{d\tau} = -4v\mathcal{F}, \quad (123)$$

$$\frac{dv}{d\tau} = \varepsilon \left\{ -\frac{\rho_{m,end}}{\mathcal{F}_{end}^{\frac{3(w_m+1)}{4}}} (3w_m + 1) \mathcal{F}^{\frac{3w_m+1}{4}} + \mathcal{F}^{\frac{1}{4}(3A+1)} \left( \beta \mathcal{F}^{\frac{3}{4}\alpha(A+1)} + 1 \right)^{-\frac{\alpha+1}{\alpha}} \left( 2\beta \mathcal{F}^{\frac{3}{4}\alpha(A+1)} - 3A - 1 \right) \right\}, \quad (124)$$

where

$$\varepsilon := \frac{1}{12\sqrt{\mathcal{F}_{end}}}. \quad (125)$$

For the numerical analysis of system (123) and (124) we select the parameter values  $\alpha \in \{0.5, 1., 1.5\}$  with  $A \in \{-0.985, -0.965, -0.945\}$ . Moreover, according to our previous estimations, for the theoretical prior  $z_{end} \simeq 10^{-2} z_{GUT}$ , we have  $5 \times 10^{23} \text{cm}^{-2} \lesssim \mathcal{F}_{end} \lesssim 5 \times 10^{37} \text{cm}^{-2}$ . Furthermore, from equations (106) and (46), we have

$$\rho_{m,end} = \rho_{m,0} \left( \frac{a_0}{a_{end}} \right)^{3(1+w_m)} = 3H_0^2 \Omega_{m,0} (1 + z_{end})^{3(1+w_m)}. \quad (126)$$

We consider dust matter ( $w_m = 0$ ) and assume  $\beta = 1$ . Next, using  $H_0 = h \cdot 1.08 \times 10^{-30} \text{cm}^{-1}$ , where  $h = (67.4 \pm 0.5) \times 10^{-2}$ ,  $\Omega_{m0} = 0.315 \pm 0.007$  and  $N_{\text{eff}} = 2.99 \pm 0.17$  according to the Planck 2018 results [122], and considering the theoretical prior  $z_{\text{end}} \simeq 10^{-2} z_{\text{GUT}}$ , we have  $4.8 \times 10^{17} \text{cm}^{-2} \lesssim \rho_{m,\text{end}} \lesssim 5.2 \times 10^{17} \text{cm}^{-2}$ . We select the best-fit value  $\rho_{m,\text{end}} \simeq 5.0 \times 10^{17}$ . Then, we have  $1.17851 \times 10^{-20} \text{cm} \lesssim \varepsilon := \frac{1}{12\sqrt{\mathcal{F}_{\text{end}}}} \lesssim 1.17851 \times 10^{-13} \text{cm}$ , and for  $w_m = 0$ , we have  $2.65915 \times 10^{-11} \lesssim \frac{\rho_{m,\text{end}}}{\mathcal{F}_{\text{end}}^{\frac{3(w_m+1)}{4}}} \lesssim 0.840896$  therefore, we are in presence of a fast-slow system. As before, (123) and (124) gives the dynamics in the fast manifold. That corresponds to the “horizontal motion”  $v = v_0$  (constant), and  $\mathcal{F}(\tau) = \mathcal{F}(\tau_0)e^{-4v_0(\tau-\tau_0)}$ . This fact is confirmed numerically, by considering the parameter region

$$\alpha \in \{0.5, 1., 1.5\}, A \in \{-0.985, -0.965, -0.945\}, \mathcal{F}_{\text{end}} \in \{5 \times 10^{23}, 5 \times 10^{37}\}, w_m = 0, \beta = 1, \rho_{m,\text{end}} = 5.0 \times 10^{17}. \quad (127)$$

In figure 12 is presented the horizontal flow of the system (123) and (124) for some values in the parameter space (101) and  $\mathcal{F}_{\text{end}} = 5 \times 10^{23}$ . Moreover, in figure 13 is presented the horizontal flow of the system (123) and (124) for some values in the parameter space (127) and  $\mathcal{F}_{\text{end}} = 5 \times 10^{37}$ .

Using the slow time  $T = \varepsilon\tau$ , we have the system

$$\varepsilon \frac{d\mathcal{F}}{dT} = -4v\mathcal{F}, \quad (128)$$

$$\frac{dv}{dT} = -\frac{\rho_{m,\text{end}}}{\mathcal{F}_{\text{end}}^{\frac{3(w_m+1)}{4}}} (3w_m + 1)\mathcal{F}^{\frac{3w_m+1}{4}} + \mathcal{F}^{\frac{1}{4}(3A+1)} \left( \beta \mathcal{F}^{\frac{3}{4}\alpha(A+1)} + 1 \right)^{-\frac{\alpha+1}{\alpha}} \left( 2\beta \mathcal{F}^{\frac{3}{4}\alpha(A+1)} - 3A - 1 \right). \quad (129)$$

We can easily see that the equilibrium governs the dynamics at the slow manifold points  $(\mathcal{F}, v)$  which satisfies  $v = 0$  and

$$-\frac{\rho_{m,\text{end}}}{\mathcal{F}_{\text{end}}^{\frac{3(w_m+1)}{4}}} (3w_m + 1)\mathcal{F}^{\frac{3w_m+1}{4}} + \mathcal{F}^{\frac{1}{4}(3A+1)} \left( \beta \mathcal{F}^{\frac{3}{4}\alpha(A+1)} + 1 \right)^{-\frac{\alpha+1}{\alpha}} \left( 2\beta \mathcal{F}^{\frac{3}{4}\alpha(A+1)} - 3A - 1 \right) = 0. \quad (130)$$

### C. Evolution of normalized energy densities

Defining

$$\Omega = \frac{\mathcal{F}}{3H^2}, \quad \Omega_m = \frac{\rho_m}{3H^2}, \quad (131)$$

such that

$$\Omega f(\mathcal{F}) + \Omega_m = 1, \quad (132)$$

and taking  $\mathcal{F}$  as a dynamical variable, we obtain the dynamical system

$$\frac{d\Omega}{dN} = \Omega (4F\Omega f'(F) + 2\Omega f(F) + (3w_m + 1)\Omega_m - 2), \quad (133)$$

$$\frac{d\Omega_m}{dN} = \Omega_m (4F\Omega f'(F) + 2\Omega f(F) + (3w_m + 1)(\Omega_m - 1)), \quad (134)$$

$$\frac{d\mathcal{F}}{dN} = -4\mathcal{F}, \quad (135)$$

defined on the invariant surface (132). The above equation can be solved globally for  $\Omega_m$  and we obtain a 2D dynamical system given by

$$\frac{d\Omega}{dN} = \Omega (4\mathcal{F}\Omega f'(\mathcal{F}) + f(\mathcal{F})(1 - 3w_m)\Omega + 3w_m - 1), \quad (136)$$

$$\frac{d\mathcal{F}}{dN} = -4\mathcal{F}, \quad (137)$$

Considering the energy condition  $\rho_m \geq 0, \rho_B \geq 0$ , the phase-plane is defined by

$$\{(\Omega, \mathcal{F}) \in \mathbb{R}^2 : 0 \leq \Omega f(\mathcal{F}) \leq 1, \mathcal{F} \geq 0\}. \quad (138)$$

The system admits the equilibrium points (at the finite region of the phase space):

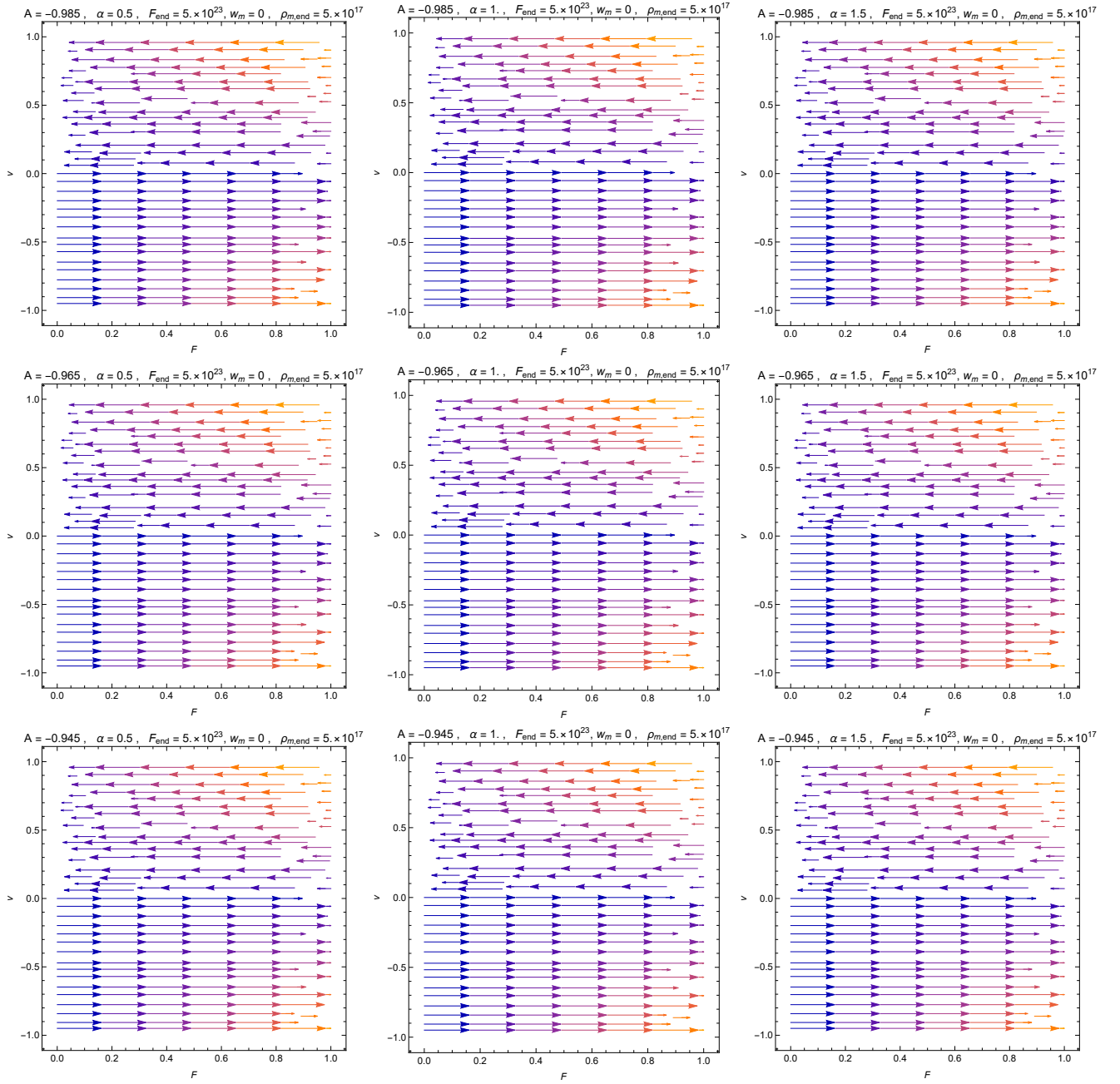


FIG. 12: Horizontal flow of the (123) and (124) for some values in the parameter space (101) and  $\mathcal{F}_{end} = 5 \times 10^{23}$

1.  $(\Omega, \mathcal{F}) = (0, 0)$ , whose eigenvalues are  $\{-4, -1 + 3w_m\}$ . It corresponds to the FRW matter dominated solution, that it is a sink for  $w_m < \frac{1}{3}$  or a saddle for  $w_m > \frac{1}{3}$ .
2.  $(\Omega, \mathcal{F}) = \left(\frac{1}{f(0)}, 0\right)$ . The eigenvalues are  $\{-4, 1 - 3w_m\}$  that it is a saddle for  $w_m < \frac{1}{3}$  or a sink for  $w_m > \frac{1}{3}$ .

According to the specific form of  $f$ , we have equilibrium points at the infinite region of the phase space or other structures like periodic solutions.



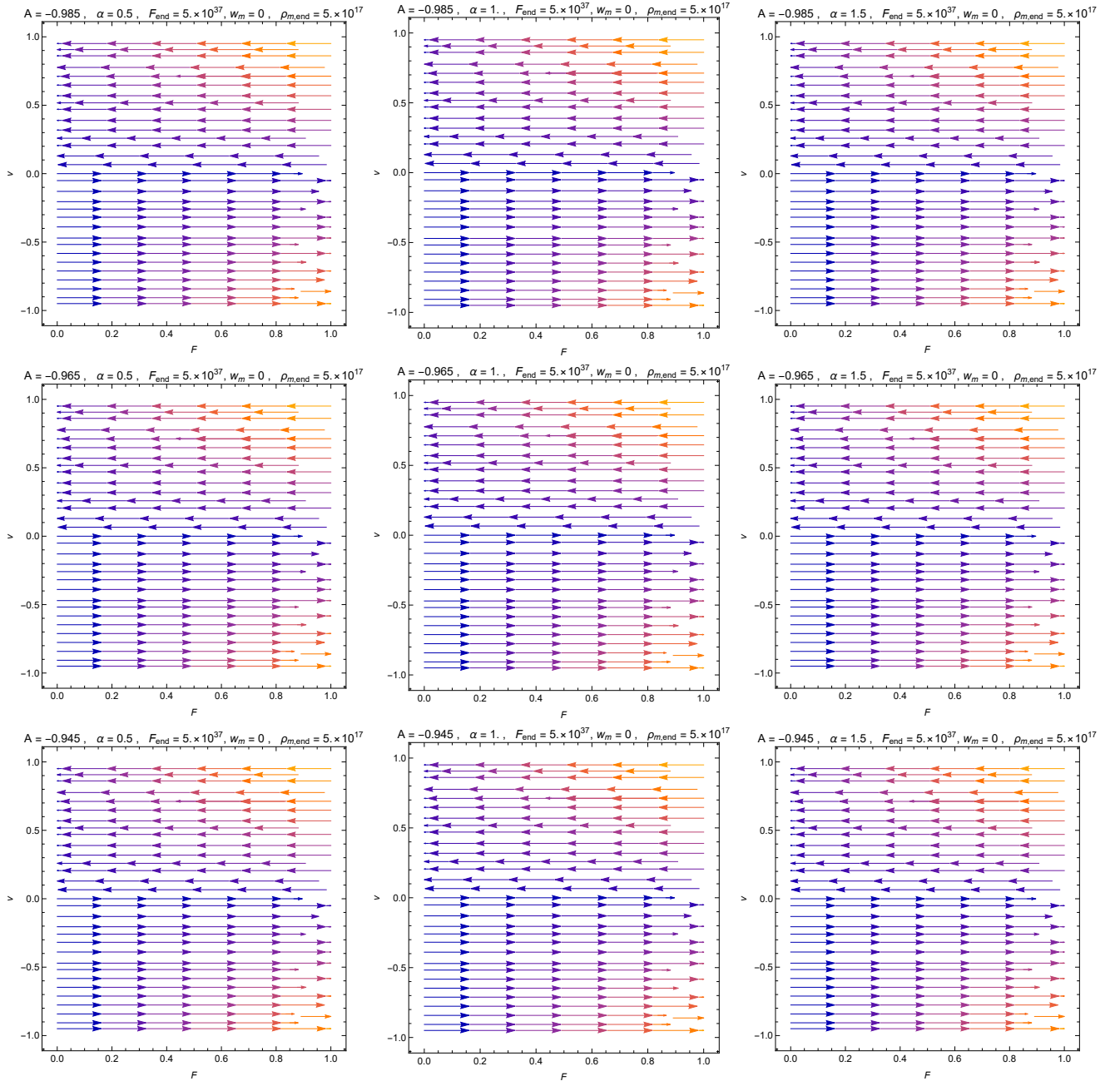


FIG. 13: Horizontal flow of the system (123) and (124) for some values in the parameter space (101) and  $\mathcal{F}_{end} = 5 \times 10^{37}$

We apply the procedure to the present model (54), such that we obtain the dynamical system

$$\begin{aligned} \frac{d\Omega}{dN} = & \Omega \left( \beta \mathcal{F}^{\frac{3}{4}\alpha(A+1)} + 1 \right)^{-\frac{\alpha+1}{\alpha}} \left( -3\beta(w_m + 1)\Omega \mathcal{F}^{\frac{3}{4}(\alpha+\alpha A+A)-\frac{1}{4}} + \beta(3w_m - 1)\mathcal{F}^{\frac{3}{4}\alpha(A+1)} \left( \beta \mathcal{F}^{\frac{3}{4}\alpha(A+1)} + 1 \right)^{\frac{1}{\alpha}} \right. \\ & \left. + (3w_m - 1) \left( \beta \mathcal{F}^{\frac{3}{4}\alpha(A+1)} + 1 \right)^{\frac{1}{\alpha}} + 3\Omega \mathcal{F}^{\frac{3A}{4}-\frac{1}{4}}(A - w_m) \right), \end{aligned} \quad (139)$$

$$\frac{d\mathcal{F}}{dN} = -4\mathcal{F}. \quad (140)$$

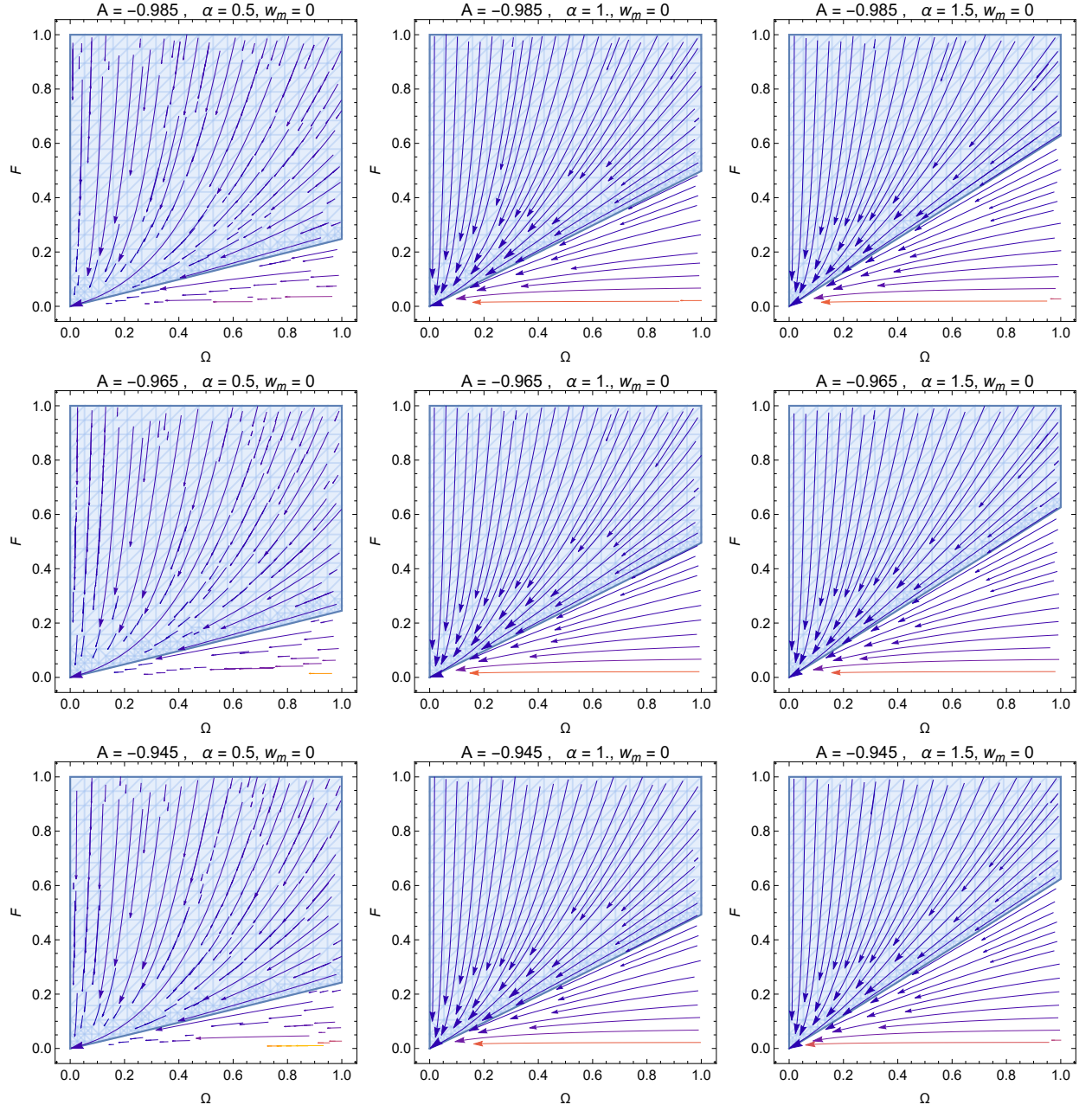


FIG. 14: A phase plot of system (139)-(140) for the region of parameters (142). The shadowed region correspond to the physical conditions  $0 \leq \Omega \mathcal{F}^{\frac{1}{4}(3A-1)} \left( \beta \mathcal{F}^{\frac{3}{4}\alpha(A+1)} + 1 \right)^{-1/\alpha} \leq 1, \mathcal{F} \geq 0$

defined on the phase space

$$\left\{ (\Omega, \mathcal{F}) \in \mathbb{R}^2 : 0 \leq \Omega \mathcal{F}^{\frac{1}{4}(3A-1)} \left( \beta \mathcal{F}^{\frac{3}{4}\alpha(A+1)} + 1 \right)^{-1/\alpha} \leq 1, \mathcal{F} \geq 0 \right\}. \quad (141)$$

We consider the parameter region

$$\alpha \in \{0.5, 1., 1.5\}, A \in \{-0.985, -0.965, -0.945\}, \beta = 1, w_m = 0. \quad (142)$$

In figure 14, we draw a phase plot of system (139)-(140) for the region of parameters (142). The attractor corresponds to the FLRW matter dominated solution that is a sink.

#### IV. CONCLUSIONS

In the present work, we have investigated the inflation driven by a non-linear electromagnetic field based on a NLED lagrangian density  $\mathcal{L}_{nled} = -\mathcal{F}f(\mathcal{F})$ , where  $f(\mathcal{F})$  is a generalized functional depending on  $\mathcal{F}$  that encodes non-linearity. We formulated an  $f$ -NLED cosmological model with a more general functional  $f(\mathcal{F})$  and showed that all NLED models can be expressed in this framework; then, we investigate in details two interesting examples of functional  $f(\mathcal{F})$ . We presented our phenomenological model based on a new Lagrangian for NLED. Solutions to the field equations with the physical properties of the cosmological parameters were obtained. We have shown that the early Universe had no Big-Bang singularity and tended to accelerate in the past. We also investigate the qualitative implications of NLED by studying the inflationary parameters, like the slow-roll parameters, spectral index  $n_s$ , and tensor-to-scalar ratio  $r$  and compare our results with observational data. Detailed phase-space analysis of our NLED cosmological model was performed with and without matter. We have examined the dynamics of our model by using dynamical systems tools.

As a first approach, we have considered the motion of a particle of the unit mass in the effective potential. This equation is satisfied on the zero-energy level, where  $\rho_B$  plays the role of effective energy density parameterized through the scale factor  $a(t)$ . Therefore, the standard cosmological model can be represented in terms of a dynamical system of a Newtonian type under a given potential  $W(u)$ . Thus,  $\frac{v^2}{2} + W(u) = E$ , is the constant of energy. Generically, the equilibrium points of the resulting system are situated on the axis  $u$  ( $v = 0$ ), and they satisfy  $\frac{\partial W(u)}{\partial u} = 0$ . From the characteristic equation, it follows that just three types of equilibrium points are admitted:

1. Saddle if  $u_c : \frac{\partial W}{\partial u}|_{u=u_c} = 0$  and  $\frac{\partial^2 W}{\partial u^2}|_{u=u_c} < 0$ ;
2. Focus if  $u_c : \frac{\partial W}{\partial u}|_{u=u_c} = 0$  and  $\frac{\partial^2 W}{\partial u^2}|_{u=u_c} > 0$ ;
3. Degenerated critical point if  $u_c : \frac{\partial W}{\partial u}|_{u=u_c} = 0$  and  $\frac{\partial^2 W}{\partial u^2}|_{u=u_c} = 0$ .

This heuristic analysis determines the dynamics on the slow manifold. Indeed, in the vacuum case we have obtained the system (97) and (98) and considered the parameter values  $\alpha \in \{0.5, 1.0, 1.5\}$  with  $A \in \{-0.985, -0.965, -0.945\}$  and  $\beta = 1$ . Moreover, according to our estimations, for the theoretical prior  $z_{end} \simeq 10^{-2} z_{GUT}$ , we have  $5 \times 10^{23} \text{cm}^{-2} \lesssim \mathcal{F}_{end} \lesssim 5 \times 10^{37} \text{cm}^{-2}$ . Then, we have  $1.17851 \times 10^{-20} \text{cm} \lesssim \varepsilon := \frac{1}{12\sqrt{\mathcal{F}_{end}}} \lesssim 1.17851 \times 10^{-13} \text{cm}$ , therefore, we are in presence of a fast-slow system. The system (97) and (98) gives the dynamics in the fast manifold. That corresponds to the “horizontal motion”  $v = v_0$  (constant), and

$$\mathcal{F}(\tau_0)e^{-4v_0(\tau-\tau_0)}. \quad (143)$$

This fact is confirmed numerically, by considering the parameter region (101). For vacuum, the dynamics at the slow manifold is governed by the equilibrium points  $(\mathcal{F}, v)$  which satisfies  $v = 0$  and

$$\left(\beta\mathcal{F}^{\frac{3}{4}\alpha(A+1)} + 1\right)^{-\frac{\alpha+1}{\alpha}} \left(2\beta\mathcal{F}^{\frac{3}{4}\alpha(A+1)} - 3A - 1\right) = 0. \quad (144)$$

That is, depending on the parameter values, the attractors are  $P_0$  or  $P_1$ . They were analyzed before in the coordinates  $(u, v)$ . Notice that the axis  $(\mathcal{F}, v) = (0, v_c)$  is a line of equilibrium points, with eigenvalues  $\{0, -4v_c\}$ .

In an analogous way, we analyzed the matter case with dust matter ( $w_m = 0$ ) and we assumed  $\beta = 1$ . Using  $H_0 = h 1.08 \times 10^{-30} \text{cm}^{-1}$ , where  $h = (67.4 \pm 0.5) \times 10^{-2}$ ,  $\Omega_{m0} = 0.315 \pm 0.007$  and  $N_{\text{eff}} = 2.99 \pm 0.17$  according to the Planck 2018 results [122], and considering the theoretical prior  $z_{end} \simeq 10^{-2} z_{GUT}$ , we have  $4.8 \times 10^{17} \text{cm}^{-2} \lesssim \rho_{m,end} \lesssim 5.2 \times 10^{17} \text{cm}^{-2}$ . We select the best-fit value  $\rho_{m,end} \simeq 5.0 \times 10^{17}$ . Then, we have  $1.17851 \times 10^{-20} \text{cm} \lesssim \varepsilon := \frac{1}{12\sqrt{\mathcal{F}_{end}}} \lesssim 1.17851 \times 10^{-13} \text{cm}$ , and for  $w_m = 0$ , we have  $2.65915 \times 10^{-11} \lesssim \frac{\rho_{m,end}}{\mathcal{F}_{end}^{\frac{3(w_m+1)}{4}}} \lesssim 0.840896$ . Therefore, we are in presence of a fast-slow system. As before, (123) and (124) determine the dynamics in the fast manifold. That corresponds to the “horizontal motion”  $v = v_0$  (constant), and  $\mathcal{F}(\tau)$  given by (143). This fact is confirmed numerically, by considering the parameter region (127). The dynamics at the slow manifold is governed by the equilibrium points  $(\mathcal{F}, v)$  which satisfies  $v = 0$  and (144) is generalized to

$$-\frac{\rho_{m,end}}{\mathcal{F}_{end}^{\frac{3(w_m+1)}{4}}}(3w_m + 1)\mathcal{F}^{\frac{3w_m+1}{4}} + \mathcal{F}^{\frac{1}{4}(3A+1)} \left(\beta\mathcal{F}^{\frac{3}{4}\alpha(A+1)} + 1\right)^{-\frac{\alpha+1}{\alpha}} \left(2\beta\mathcal{F}^{\frac{3}{4}\alpha(A+1)} - 3A - 1\right) = 0. \quad (145)$$

Due to the difficulties in analyzing the fast-slow dynamics, and the dependence on the observed parameters  $\mathcal{F}_{end}, \rho_{m,end}$  etc., we have considered alternative Hubble-normalized variables (131). In the general case, the system admitted the equilibrium points (at the finite region of the phase space): (i)  $(\Omega, \mathcal{F}) = (0, 0)$ , whose eigenvalues

are  $\{-4, -1 + 3w_m\}$ . It corresponds to the FLRW matter dominated solution, that it is a sink for  $w_m < \frac{1}{3}$  or a saddle for  $w_m > \frac{1}{3}$ ; and (ii)  $(\Omega, \mathcal{F}) = \left(\frac{1}{f(0)}, 0\right)$ . The eigenvalues are  $\{-4, 1 - 3w_m\}$  that it is a saddle for  $w_m < \frac{1}{3}$  or a sink for  $w_m > \frac{1}{3}$ . In the particular case of  $f(\mathcal{F})$  in (54) we have obtained the system (139) and (140) where the late-time attractor is the FRW matter dominated solution  $(\Omega, \mathcal{F}) = (0, 0)$ . The last analysis complemented the analysis of the fast-slow dynamics.

### Acknowledgments

HBB gratefully acknowledges the financial support from University of Sharjah. The work of HQ was partially supported by UNAM-DGAPA-PAPIIT, Grant No. 114520, and Conacyt-Mexico, Grant No. A1-S-31269. The research of Genly Leon is funded by Vicerrectoría de Investigación y Desarrollo Tecnológico (Vridt) at Universidad Católica del Norte. He also thanks Vridt support through Concurso De Pasantías De Investigación Año 2022, Resolución Vridt N°040/2022.

- 
- [1] A. A. Starobinsky, Phys. Lett. B **91**, 99-102 (1980)
  - [2] A.H. Guth, Phys. Rev. D **23**, 347 (1981)
  - [3] A.D. Linde, Phys. Lett. B **108**, 389 (1982)
  - [4] A. Albrecht, P.J. Steinhardt, Phys. Rev Lett. **48**, 1220 (1982)
  - [5] L. Abbott, M.B. Wise, Nucl. Phys. B **244**, 541 (1984)
  - [6] F. Lucchin, S. Matarrese, Phys. Rev. D **32**, 1316 (1985)
  - [7] A. R. Ade et al., Planck Collaboration (Planck 2013 results. XXII. Constraints on inflation), Astron. Astrophys. **571**, A22 (2014)
  - [8] P. A. R. Ade et al., Planck Collaboration (Planck 2015 results. XX. Constraints on inflation), Astron. Astrophys. **594**, A20 (2016);
  - [9] Y. Akrami et al., Planck Collaboration (Planck 2018 results. X. Constraints on inflation), Astron. Astrophys. **641**, A10 (2020)
  - [10] P.A.R. Ade et al., A joint analysis of BICEP2/Keck array and planck data. Phys. Rev. Lett. **114**, 101301 (2015).
  - [11] Y. Akrami et al., Planck Collaboration (Planck 2018 results. IX. Constraints on primordial non-Gaussianity), Astron. Astrophys. **641**, A9 (2020)
  - [12] Fedor L. Bezrukov, Mikhail Shaposhnikov, Phys. Lett. B **659**, 703–706 (2008).
  - [13] S. Nojiri, S. D. Odintsov and V. K. Oikonomou, Phys. Rept. **692**, 1 (2017).
  - [14] G. Leon and E. N. Saridakis, JCAP **0911**, 006 (2009).
  - [15] C. Xu, E. N. Saridakis and G. Leon, JCAP **1207**, 005 (2012).
  - [16] G. Leon and E. N. Saridakis, JCAP **1303**, 025 (2013).
  - [17] G. Leon, J. Saavedra and E. N. Saridakis, Class. Quant. Grav. **30**, 135001 (2013).
  - [18] G. Kofinas, G. Leon and E. N. Saridakis, Class. Quant. Grav. **31**, 175011 (2014).
  - [19] G. Leon, Y. Leyva and J. Socorro, Phys. Lett. B **732**, 285 (2014).
  - [20] C. R. Fadrakas, G. Leon and E. N. Saridakis, Class. Quant. Grav. **31**, 075018 (2014).
  - [21] G. Leon and E. N. Saridakis, JCAP **1511**, no. 11, 009 (2015).
  - [22] G. Pulgar, J. Saavedra, G. Leon and Y. Leyva, JCAP **1505**, 046 (2015).
  - [23] G. Leon and E. N. Saridakis, JCAP **1504**, no. 04, 031 (2015).
  - [24] A. Giacomini, S. Jamal, G. Leon, A. Paliathanasis and J. Saavedra, Phys. Rev. D **95**, no. 12, 124060 (2017).
  - [25] E. Aydiner, Sci. Rep. **8**, no. 1, 721 (2018).
  - [26] A. Joyce, L. Lombriser and F. Schmidt, Ann. Rev. Nucl. Part. Sci. **66**, 95 (2016).
  - [27] S. Tsujikawa, Class. Quant. Grav. **30**, 214003 (2013).
  - [28] S. Lepe, G. Otalora and J. Saavedra, Phys. Rev. D **96**, no. 2, 023536 (2017).
  - [29] T. Harko, F. S. N. Lobo, G. Otalora and E. N. Saridakis, JCAP **1412**, 021 (2014).
  - [30] G. Otalora, Phys. Rev. D **88**, 063505 (2013).
  - [31] G. Otalora, JCAP **1307**, 044 (2013).
  - [32] G. Otalora, A. Övgün, J. Saavedra and N. Videla, JCAP **1806**, no. 06, 003 (2018).
  - [33] H. Azri and D. Demir, Phys. Rev. D **97**, no.4, 044025 (2018).
  - [34] H. Azri and D. Demir, Phys. Rev. D **95**, no.12, 124007 (2017).
  - [35] F. Bauer and D. A. Demir, Phys. Lett. B **698**, 425-429 (2011).
  - [36] İ. İ. Çimdiker, Phys. Dark Univ. **30**, 100736 (2020).
  - [37] E. Guendelman, R. Herrera and D. Benisty, Phys. Rev. D **105**, no.12, 124035 (2022).
  - [38] L. Aresté Saló, D. Benisty, E. I. Guendelman and J. de Haro, Phys. Rev. D **103**, no.12, 123535 (2021).
  - [39] L. Aresté Saló, D. Benisty, E. I. Guendelman and J. d. Haro, JCAP **07**, 007 (2021).
  - [40] D. Benisty and E. I. Guendelman, Eur. Phys. J. C **80**, no.6, 577 (2020).

- [41] G. Lambiase, PoS **DSU2015**, 012 (2016).
- [42] S. Capozziello, G. Lambiase and H. J. Schmidt, *Annalen Phys.* **9**, 39-48 (2000).
- [43] S. Vagnozzi, *Mon. Not. Roy. Astron. Soc.* **502**, no.1, L11-L15 (2021).
- [44] R. Myrzakulov, L. Sebastiani and S. Vagnozzi, *Eur. Phys. J. C* **75**, 444 (2015).
- [45] J. D. Barrow, *Phys. Lett.* **B235** (1990) 40–43.
- [46] J. D. Barrow and P. Saich, *Phys. Lett.* **B249** (1990) 406–410.
- [47] J. D. Barrow and A. R. Liddle, *Phys. Rev.* **D47** (1993) 5219–5223,
- [48] J. D. Barrow and N. J. Nunes, *Phys. Rev.* **D76** (2007) 043501,
- [49] S. del Campo and R. Herrera, *JCAP* **0904** (2009) 005,
- [50] R. Herrera and N. Videla, *Eur. Phys. J.* **C67** (2010) 499–505,
- [51] R. Herrera, M. Olivares and N. Videla, *Eur. Phys. J.* **C73** (2013) 2295,
- [52] R. Herrera, M. Olivares and N. Videla, *Eur. Phys. J.* **C73** (2013) 2475,
- [53] R. Herrera, M. Olivares and N. Videla, *Int. J. Mod. Phys.* **D23** (2014) 1450080,
- [54] R. Herrera, N. Videla and M. Olivares, *Eur. Phys. J.* **C75** (2015) 205,
- [55] A. Cid, G. Leon and Y. Leyva, *JCAP* **1602**, no. 02, 027 (2016)
- [56] M. Kierdorf et al., *Astronomy & Astrophysics* **600**, id.A18 (2017).
- [57] R. Jimenez and A. Loeb, *Astrophys. J.* **573**, 37 (2002).
- [58] Moresco, M., Cimatti, A., Jimenez, R., et al. 2012, *JCAP*, 8, 006.
- [59] A.A. Sen and R.J Scherrer, *Phys. Rev. D* **72** , 063511 (2005).
- [60] E.O. Kahya, B. Pourhassan and S. Uraz, *Phys. Rev. D* **92** , 103511 (2015).
- [61] S. del Campo, *JCAP* **2013**, 004 (2013).
- [62] S. M. Carroll, *Living Rev.Rel.* **4**, 1 (2001).
- [63] S. W. Hawking, *Phys. Rev. Lett.* **17**, 444 (1966).
- [64] V. F. Mukhanov and R. H. Brandenberger, *Phys. Rev. Lett.* **68**, 1969 (1992).
- [65] M. Novello, S. E. Perez Bergliaffa and J. M. Salim, *Class. Quant. Grav.* **17**, 3821 (2000)
- [66] B. Shahid-Saless, 1990, *J. Math. Phys.* **31**, 2429 (1990) .
- [67] R.H. Brandenberger, V.F. Mukhanov and A. Sornborger, *Phys. Rev. D* **48**, 1629 (1993).
- [68] Y.-F. Cai, D.A. Easson and R. Brandenberger, *JCAP* **08**, 020 (2012) 020.
- [69] M. Trodden, V. F. Mukhanov, and R. H. Brandenberger, *Phys. Lett. B* **316**, 483 (1993) .
- [70] M. Born, *Nature* 132 (1933): 282-282.
- [71] M. Born, *Proc. R. Soc. A* 143 (1934) 410.
- [72] M. Born, L. Infeld, *Proc. R. Soc. A* 144 (1934) 425.
- [73] S. A. Gutierrez, A. L. Dudley and J. F. Plebanski, *J. Math. Phys.* **22**, 2835-2848 (1981); J.F. Plebanski, *Lectures on nonlinear electrodynamics*, monograph of the Niels Bohr Institute (Nordita,Copenhagen, 1968).
- [74] H. J. Mosquera Cuesta and G. Lambiase, *Phys. Rev. D* **80**, 023013 (2009).
- [75] C. Corda and H. J. Mosquera Cuesta, *Astropart. Phys.* **34**, 587-590 (2011).
- [76] H. J. Mosquera Cuesta, G. Lambiase and J. P. Pereira, *Phys. Rev. D* **95**, no.2, 025011 (2017),
- [77] C. Baccigalupi, F. Perrotta, G. De Zotti, G. F. Smoot, C. Burigana, D. Maino, L. Bedini and E. Salerno, *Mon. Not. Roy. Astron. Soc.* **354**, 55-70 (2004).
- [78] H. J. Mosquera Cuesta and J. M. Salim, *Astrophys. J.* **608**, 925-929 (2004).
- [79] H. J. Mosquera Cuesta, J. A. de Freitas Pacheco and J. M. Salim, *Int. J. Mod. Phys. A* **21**, 43-55 (2006).
- [80] J. P. Mbelek, H. J. Mosquera Cuesta, M. Novello and J. M. Salim, *EPL* **77**, no.1, 19001 (2007).
- [81] J. P. Mbelek and H. J. Mosquera Cuesta, *Mon. Not. Roy. Astron. Soc.* **389**, 199 (2008).
- [82] J. Lundin, G. Brodin and M. Marklund, *Phys. Plasmas* **13**, 102102 (2006).
- [83] M. Marklund and P. K. Shukla, *Rev. Mod. Phys.* **78**, 591-640 (2006).
- [84] D. H. Delphenich, [arXiv:hep-th/0610088 [hep-th]].
- [85] E. Lundstrom, G. Brodin, J. Lundin, M. Marklund, R. Bingham, J. Collier, J. T. Mendonca and P. Norreys, *Phys. Rev. Lett.* **96**, 083602 (2006).
- [86] Y. Akamatsu and N. Yamamoto, *Phys. Rev. Lett.* **111**, 052002 (2013).
- [87] S. I. Kruglov, *Phys.Rev. D* **92**, no.12, 123523 (2015).
- [88] S. I. Kruglov, *Int. J. Mod. Phys. D* **25**, no. 4, 1640002 (2016).
- [89] S. I. Kruglov, *Int. J. Mod. Phys. A* **32**, 13, 1750071 (2017).
- [90] A. Övgün, *Eur. Phys. J. C* **77**, no. 2, 105 (2017)
- [91] M. Sharif and S. Mumtaz, *Eur.Phys.J. C* **77**, no.2, 136 (2017).
- [92] R. Durrer, A. Neronov, *Astron Astrophys Rev* **21**, 62, (2013).
- [93] R. Garcia-Salcedo, T. Gonzalez, I. Quiros, *Phys.Rev. D* **89**, 084047 (2014).
- [94] M. Novello, et al. *Phys.Rev. D* **69**, 127301 (2004).
- [95] M. Novello, et al. *Class.Quant.Grav.* **24**, 3021-3036 (2007).
- [96] D. N.Vollick, *Phys.Rev. D* **78**, 063524 (2008).
- [97] M. Novello, S.E.P. Bergliaffa, *Phys.Rept.* **463**, 127-213 (2008).
- [98] V.F. Antunes, M. Novello, *Grav.Cosmol.* **22**, no.1, 1-9 (2016).
- [99] E. Bittencourt, U. Moschella, M. Novello, J.D. Toniato, *Phys.Rev. D* **90**, no.12, 123540 (2014).
- [100] K. E. Kunze, *Plasma Phys.Control.Fusion* **55**, 124026 (2013).
- [101] K. E. Kunze, *Phys.Rev. D* **77**, 023530 (2008).

- [102] L. Campanelli, P. Cea, G. L. Fogli and L. Tedesco, Phys. Rev. D **77**, 043001 (2008).
- [103] V. A. De Lorenci, R. Klippert, M. Novello and J. M. Salim, Phys. Rev. D **65**, 063501 (2002).
- [104] S.I. Kruglov Annals of Physics 353 (2015) 299-306.
- [105] M. Novello, E. Goulart, J. M. Salim, S. E. Perez Bergliaffa, Class. Quantum Grav. **24** (2007) 3021-3036
- [106] M. Aiello, G. R. Bengochea, and R. Ferraro, 2008, JCAP, **6**, 006
- [107] L. Medeiros, Int.J.Mod.Phys. D23, 1250073 (2012),1209.1124.
- [108] A. Montiel, N. Breton and V. Salzano, Gen. Rel. Grav. **46**, 1758 (2014)
- [109] A. Övgün, G. Leon, J. Magaña and K. Jusufi, Eur. Phys. J. C (2018) 78:462.
- [110] R. Garcia-Salcedo and N. Breton, Class. Quant. Grav. **20**, 5425 (2003)
- [111] Sergey I. Kruglov. Universe 2018, 4(5), 66.
- [112] S.I. Kruglov, Int. J. Mod. Phys. A 2018, 33, 1850023.
- [113] H.B. Benaoum and A. Övgün, Class.Quant. Grav. **38**, 135019 (2021).
- [114] A. Neronov and I. Vovk, Science **328**, 73 (2010).
- [115] A. M. Taylor, I. Vovk, and A. Neronov, A&A **529**, A14 (2011) .
- [116] Ade, P.A.R., et al.: Planck 2015 Results. XIX. Constraints on Primordial Magnetic Fields. A&A 594, A19 (2016).
- [117] Anwar S. AlMuhammad, Rafael Lopez-Mobilia, Gen Relativ Gravit (2015) 47:134.
- [118] D. Grasso and H. R. Rubinstein, Phys. Rept. **348**, 163 (2001).
- [119] K. Subramanian, Rep. Prog. Phys. **79**, 076901 (2016).
- [120] H. J. Mosquera Cuesta and G. Lambiase, JCAP **03**, 033 (2011).
- [121] R. Tolman, P. Ehrenfest, Phys.Rev. **36**, no.12, 1791 (1930).
- [122] N. Aghanim *et al.* [Planck], Astron. Astrophys. **641** (2020), A6 doi:10.1051/0004-6361/201833910
- [123] A. G. Riess et al., A.J. **116** 1009-1038 (1988).
- [124] J. Wainwright and G. F. R. Ellis. Dynamical Systems in Cosmology. Cambridge University Press, 1997.
- [125] A. A. Coley, "Dynamical systems and cosmology", Vol. 291, Kluwer, Dordrecht, Netherlands, 2003 .
- [126] A. Alho, J. Hell and C. Ugla, Class. Quant. Grav. **32**, no.14, 145005 (2015).
- [127] A. Alho, V. Bessa and F. C. Mena, J. Math. Phys. **61**, no.3, 032502 (2020).
- [128] D. Fajman, G. Heißel and M. Maliborski, Class. Quant. Grav. **37**, no.13, 135009 (2020).
- [129] G. Leon, E. González, S. Lepe, C. Michea and A. D. Millano, Eur. Phys. J. C **81**, no.5, 414 (2021) [erratum: Eur. Phys. J. C **81**, no.12, 1097 (2021)].
- [130] G. Leon, S. Cuellar, E. Gonzalez, S. Lepe, C. Michea and A. D. Millano, Eur. Phys. J. C **81**, no.6, 489 (2021) [erratum: Eur. Phys. J. C **81**, no.12, 1100 (2021)].
- [131] D. Fajman, G. Heißel and J. W. Jang, Class. Quant. Grav. **38**, no.8, 085005 (2021).
- [132] S. Chakraborty, E. González, G. Leon and B. Wang, Eur. Phys. J. C **81**, no.11, 1039 (2021).
- [133] F. Dumortier and R. Roussarie, (Memoirs of the American Mathematical Society, 577).
- [134] N. Fenichel, Journal of Differential Equations **31**, 53-98 (1979).
- [135] G. Fusco and J.K. Hale, Journal of Dynamics and Differential Equations **1**, 75 (1988).
- [136] N. Berglund and B. Gentz, "Noise-Induced Phenomena in Slow-Fast Dynamical Systems", Series: Probability and Applications, Springer-Verlag: London, (2006).
- [137] M. H. Holmes (2013) "Introduction to Perturbation Methods", (Springer Science+Business Media New York, ISBN 978-1-4614-5477-9)
- [138] Jirair Kevorkian, J.D. Cole (1981) "Perturbation Methods in Applied Mathematics" (Applied Mathematical Sciences Series, Volume 34 (Springer-Verlag New York eBook ISBN 978-1-4757-4213-8)
- [139] Ferdinand Verhulst, (2000) "Methods and Applications of Singular Perturbations: Boundary Layers and Multiple Timescale Dynamics" (Springer-Verlag New York, ISBN 978-0-387-22966-9)